IN VIVO AND IN VITRO EFFECTS OF IVERMECTIN TREATMENT ON BRUGIA MALAYI MICROFILARIAE

by

ASHLEY MEGAN ROGERS

(Under the Direction of Adrian J. Wolstenholme)

ABSTRACT

Wuchereria bancrofti, Brugia malayi, and *B. timori*, are filarial nematodes that cause lymphatic filariasis, an extremely debilitating disease, which is prevalent in the developing world. Current control is based on mass drug administration with annual doses, under a two-drug regimen. One of these drugs, ivermectin, has been considered a wonder drug since its discovery, but its mode of action in filarial nematodes is still unclear. Currently, ivermectin is thought to decrease helminth-immunomodulation by inhibiting protein secretion from the excretory/secretory pore. We performed *in vitro* motility assays, neutrophil attachment assays, and neutrophil activation assays, which suggest a role for the immune system, in conjunction with ivermectin, in clearing microfilariae from blood circulation. Also, transcriptomic analysis of microfilariae treated with ivermectin, *in vivo*, reveals gene regulation that could indicate a mode of action in filarial nematodes. Due to increasing resistance it is imperative to understand ivermectin's mode of action.

INDEX WORDS: Lymphatic filariasis, *Brugia malayi*, ivermectin, neutrophil immunomodulatory, microfilariae, *in vitro, in vivo*

IN VIVO AND IN VITRO EFFECTS OF IVERMECTIN TREATMENT ON BRUGIA MALAYI MICROFILARIAE

by

ASHLEY MEGAN ROGERS

B.S.A., The University of Georgia, 2009

A Thesis Submitted to the Graduate Faculty of The University of Georgia in Partial Fulfillment of the Requirements for the Degree

MASTER OF SCIENCE

ATHENS, GEORGIA

2013

IN VIVO AND IN VITRO EFFECTS OF IVERMECTIN TREATMENT ON BRUGIA MALAYI MICROFILARIAE

by

ASHLEY MEGAN ROGERS

Major Professor: Adrian J. Wolstenholme

Committee: Andrew R. Moorhead
David S. Peterson

Electronic Version Approved:

Maureen Grasso
Dean of the Graduate School
The University of Georgia
August 2013

DEDICATION

To my mother, Pamela Rogers, my father, William Rogers, and Tonya Rogers. Without your love and support throughout the years this could not have been possible. Thank you for all of the encouragement to follow my dreams, wherever they may take me. To you I am truly grateful.

ACKNOWLEDGEMENTS

My accomplishments over the past two years would have never come to fruition without the constant guidance of my mentor, Dr. Adrian Wolstenholme. Without him I would have no knowledge of the inner-workings of the parasitologists I've come to work with, nor the parasites themselves. His patience, humor, and love for parasitology have made my graduate career a sheer pleasure. I have also come to rely on words of wisdom from Dr. "Andy" Moorhead. His energetic personality made every day leading up to this moment well worth it. Also, without Dr. Barbara Reaves I would still be in the dark about fluorescence microscopy and without Dr. Balazs Rada I would know even less about neutrophils. I would also like to acknowledge Dr. David Peterson for providing an outside perspective on helminthology.

This work would have been impossible without constant help from all of those at the FR3. I thank Drs. Mike Dzimianski and Prasit Supakorndej, Erica Burkman, Molly Riggs, and Chris Evans for supplying me with all the microfilariae, gerbils and insight I could even need. I'd also like to thank Sue Howell and Bob Storey for all of their assistance and insight into the wonderful world of worms. Thank you to all of the gerbils used in our studies and to the funding from the NIH that created this opportunity.

A final thank you to Dr. Lee Pope for being by my side every step of the way and for always pushing me to do my best, and to Mr. and Mrs. Pope for all of their moral support and guidance.

TABLE OF CONTENTS

Page

LIST OF TABLES

Page

LIST OF FIGURES

Page

CHAPTER 1

LITERATURE REVIEW

Overview of Human Filarial Infections

Human filarial infections are caused by parasitic nematodes (roundworms) belonging to the family *Onchocercidae*. This family contains many species of which *Wuchereria bancrofti, Brugia malayi, Onchocerca volvulus*, and *Loa loa* are of importance. They cause diseases such as lymphatic filariasis (LF), river blindness, and loaisis. In 2004, it was speculated that three billion people were infected with parasites. Of those, 250 million were infected with filarial species (Gupta et al 2004). After mood disorders, filarial diseases are the most common cause of physical morbidity in the world (Shenoy et al 1999). Not only do these infections cause severe disfigurement and serious health problems, they also lead to psychosocial and psychosexual stigmas that can last a lifetime in those affected (Choi et al 2011). Despite these problematic findings, human helminthiases are considered to be one of the neglected tropical diseases (NTDs) (Boatin et al 2012).

Terms such as elephantiasis, lymphatic filariasis, loiasis, and river blindness have not always been known by witnesses of these diseases. There are no written records of the first cases of filarial infections and they are presumed to be pre-historic. The earliest indications of infection and clinical disease come from statues. The first is of Mentuhoptep II, an Egyptian Pharaoh, who is depicted with swollen limbs, dating back to 2000 BC. Other smaller statues, from 500 BC, in West Africa depict enlarged scrota,

which could be the characteristic testicular hydrocele associated with LF. The first written reports of LF, loiasis, and river blindness, previously known as *craw craw*, appeared at the end of the sixteenth and seventeenth centuries. The discovery of the life cycles and causative agents of the filarial diseases was intermittent throughout the nineteenth and twentieth centuries and paved the way for understanding how to control these parasites (Cox 2002).

Since before their discovery, filarial nematodes have been plaguing humans and animals worldwide. There is an ongoing battle with trying to control these debilitating diseases. While there are currently global eradication programs in place, there is still the question as to whether or not the knowledge, tools, and funding required to eliminate or even control human helminthiases are available (Boatin et al 2012).

Lymphatic Filariasis

Lymphatic filariasis is a disease caused by filarial helminths in developing countries (Figure 1). While the most recognizable form of LF is elephantiasis, this clinical manifestation only occurs in a small percentage of those infected. Many of those infected are often asymptomatic despite the fact that microfilariae (mf) are circulating throughout their blood and adult worms reside in their lymphatics. Elephantiasis and lymphedema can develop in cases of chronic infection where the lymphatics are obstructed by lymph thrombi, dead worms, endothelial proliferation, granulomas, and fibrin deposition (Cross 1996). These clinical manifestations are often unaccompanied by mf when the infection is no longer active. This is why elephantiasis is often seen in middle-aged adults. Symptoms of LF can range anywhere from fever, lymphadenopathy,

genital damage, to lymphedema. Diagnosis is usually by physical examination and identification of mf in a blood smear, however, this could be misleading in early and late infections where mf are not present in the blood (Brown et al 2000, Cross 1996).

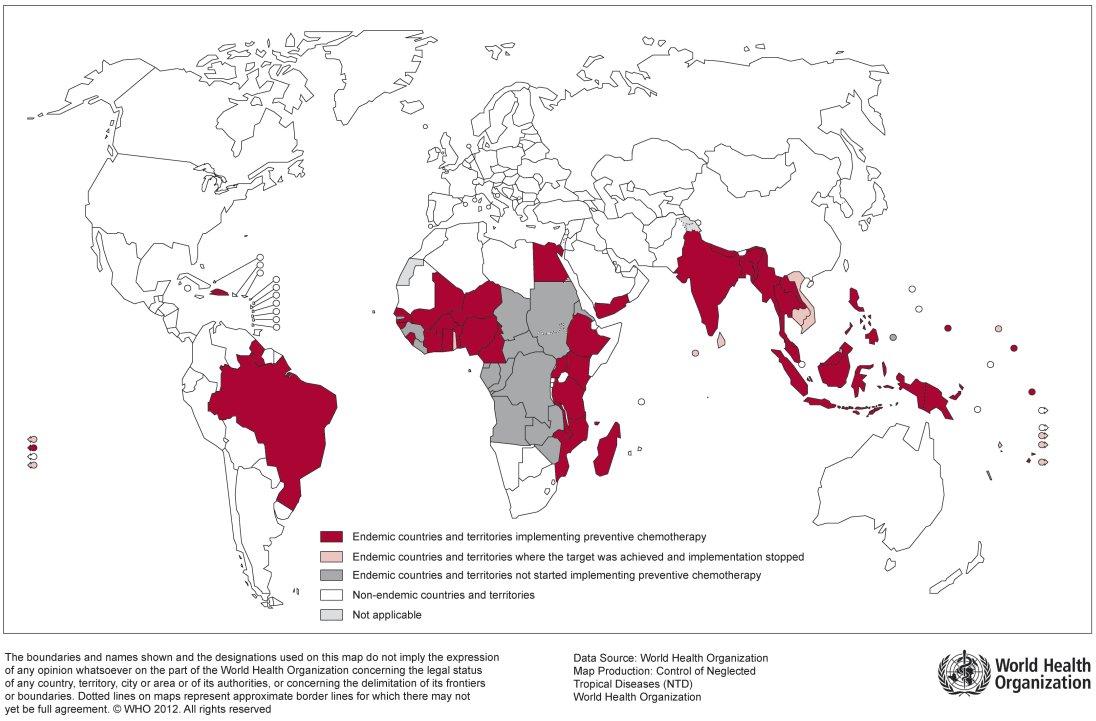

Figure 1: **WHO geographical representation of distribution and status of Mass Drug Administration for lymphatic filariasis in 2011.**

Causative Agents of Lymphatic Filariasis

There are three species of nematode that cause LF, *W. bancrofti*, *B. malayi,* and *B. timori*. The majority of the cases are caused by the first two, of which *Wuchereria bancrofti* accounts for 90% of LF cases and the remaining 10% are primarily due to infection with *B. malayi* (Genchi et al 2012). It is estimated that 120 million people in 73 countries are currently infected with the causative agents of LF and 1.4 billion people are at risk for acquiring a filarial diseases such as LF (GPELF 2012). *Brugia malayi* is endemic in Southeast Asia and Indonesia, whereas *W. bancrofti* is more prominent in

other tropical and subtropical countries (Figure 1) (Cross 1996, Ghedin et al 2007, WHO 2011). These roundworms have a complex life cycle in which they go through multiple morphological changes within two different hosts (Figure 2). Circulation of mf in the blood is sub-periodic where mf sequester in the arterioles of the lungs for the majority of the day, but at night they circulate via the blood, bettering their chances of being ingested by a biting mosquito (Hawking & Gammage 1968). *Aedes* and *Mansonai* mosquitoes are the typical vectors for *B. malayi* while *W. bancrofti* can also be transmitted by *Culex* and *Anopholes* species depending on the geographical location (CDC 2013). L3s enter the human host through the bite of an infected mosquito. They continue to mature over a period of about 10 days into a fourth stage larvae (L4) and, subsequently, after a few weeks become dioecious immature adults. After about six more weeks, the adults become sexually mature, mate, and the females produce mf that move into the peripheral blood. The mf can then be ingested by a susceptible mosquito and over 14 days they complete two molts associated with early larval development within the arthropod. Overall, these filarids undergo four molts to produce five major stages in human LF and can persist in humans for more than a decade (Bennuru et al 2009, Ghedin et al 2007, Li et al 2012, Moreno et al 2010).

Laboratory Models of Lymphatic Filariasis

One disadvantage of working with parasites that naturally infect only humans is finding an appropriate laboratory model. For LF, *B. malayi* is the only real model for human infection that can be maintained in a laboratory setting (Choi et al 2011). Another pressing matter is finding an appropriate animal that might mimic a natural infection in

humans. A proper model is considered invaluable in mechanistic studies especially for studies on helminth-induced immune responses *in vivo*. The key to developing such a model is to minimize variation in the host, the infection, and polymorphisms in the parasite that might be attributed to an inappropriate animal model. While infection is variable in humans, limiting variation in an animal model will provide a better

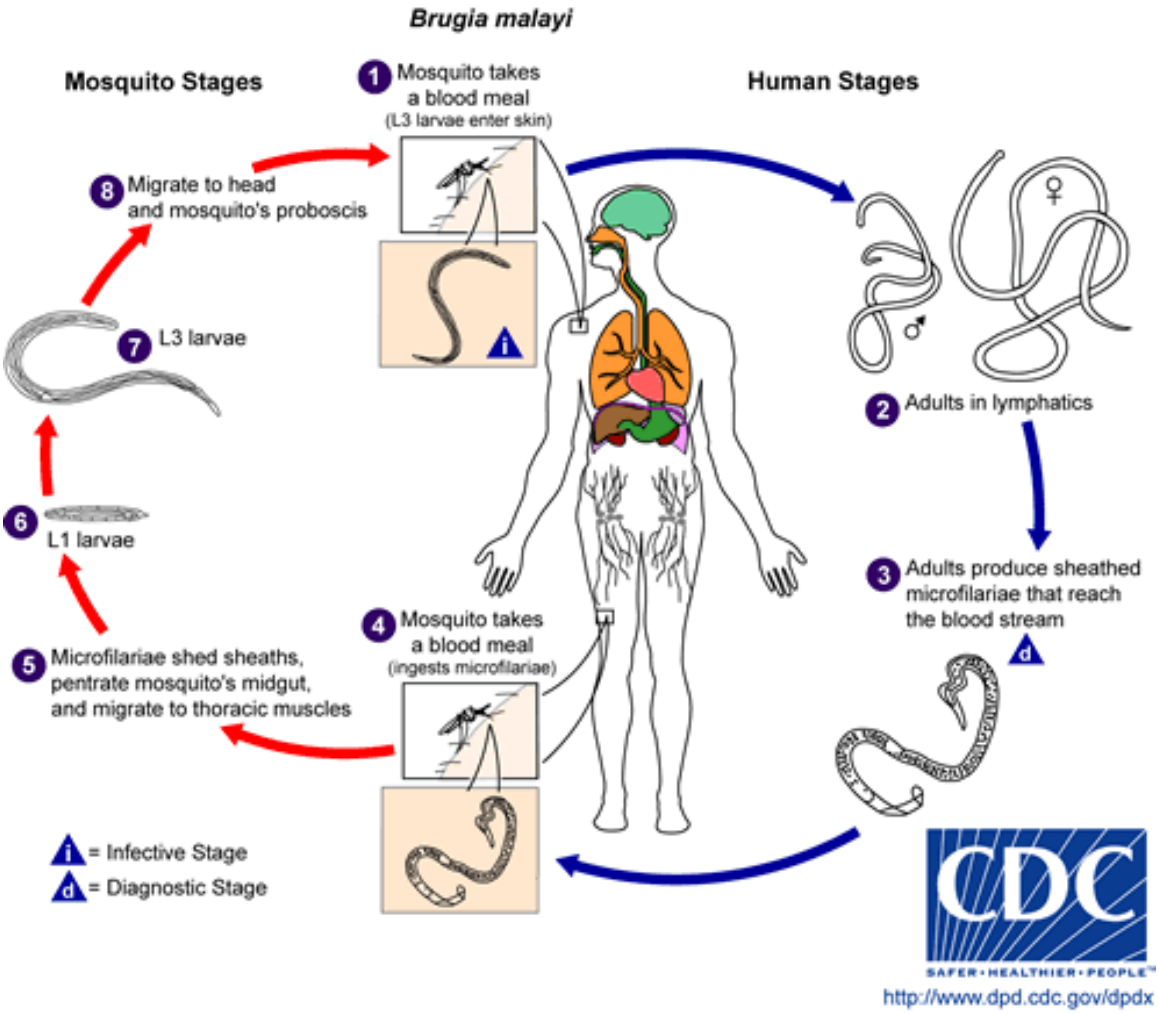

Figure 2: **CDC representation of *B. malayi* life cycle.** 1) An infected mosquito takes a blood meal and the infective third stage larvae (L3) enters through the bite wound. 2) The L3s develop into adults and reside in the lymphatics. 3) The females release thousands of mf into the lymph and they eventually circulate in the blood. 4) A mosquito takes a blood meal and ingests the mf. 5) In the mosquito the mf ex-sheath and penetrate through the midgut of the mosquito and migrate to the thoracic muscles. 6 & 7) In the midgut the mf develop into a first-stage larvae (L1) and continue to molt two times before becoming an L3. 8) The L3s migrate to the proboscis where they remain until the mosquito takes another blood meal.

understanding in context to the progression of disease. Current experimental models have not been shown to reflect the complexity of human helmith immunobiology (Bourke et al 2011). Multiple animal models have been used in studies for LF: cats, ferrets, mice, African mastomys, and gerbils to name a few (Crandall et al 1982, Grenfell et al 1991, Gupta et al 2004, Michalski et al 2011). At present, the preferred animal model for LF infection is the Mongolian gerbil (*Meriones ungiuculatus*) due to its high susceptibility to infection with *B. malayi*. Intraperitoneal injections of L3s result in completion of the life cycle and are a source of L4s, adults, and mf, while subcutaneous injections can result in lymphatic infection, similar to that seen in humans.

Mass Drug Administration to Control Transmission

In 1997 the World Health Organization (WHO) decided to take action to eliminate LF as a public problem by implementing Mass Drug Administration (MDA) (Horton et al 2000). For over 40 years, diethylcarbamazine (DEC) was the only chemotherapeutic agent used to treat filariasis due to its micro- and macrofilaricidal effects on some species. One disadvantage of using DEC was the recommended dosing regimen of 6 mg/kg over a course of 6-12 days. Not only did this cause side effects due to the rapid killing of mf, which decreased compliance, it also caused severe adverse effects, such as anaphylaxis, in those co-infected with *Onchocerca* (Brown et al 2000, Horton et al 2000). A single dose, two-drug regimen was the most effective in treating LF. Efficacy studies revealed that ivermectin (IVM) paired with DEC was the most effective regimen, but due to contraindications for DEC in areas of onchocerciasis and

IVM in areas of loaiasis these two are not paired together (Brown et al 2000, Shenoy et al 1999). In 1998, the Global Programme to Eliminate Lymphatic Filariasis (GPELF) deemed a regimen of IVM (0.2 mg/kg) with albendazole (ALB; 400 mg) or DEC (6 mg/kg) with ALB (400 mg) safe and effective for areas of high helminth co-infection (Gonzalez Canga et al 2008, Horton et al 2000). Albendazole alone did not seem to have any effect on mf, but it is a broad spectrum anthelmintic against intestinal parasites and has shown to reduce morbidity in school-aged children (Shenoy et al 1999). Side effects, such as muscle pain, headache, fever, dizziness and abdominal pain, were the most common adverse events reported in microfilaremic individuals, while the majority of afilaremic individuals did not report adverse events. Originally these side effects were thought to be associated with MDA toxicity, but have been found to be related to parasite burden and not drug toxicity. Most individuals experience the majority of their side effects upon first treatment when mf blood density is high and there is a high level of mf death (Gonzalez Canga et al 2008, Horton et al 2000, Ottesen et al 1990).

Ivermectin

Ivermectin is one of the drugs used today to control many kinds of nematode infections in both animals and humans. Since the discovery, in 1970, of the natural form it has been termed a 'wonder drug'. In a figure from Crump and Omura (2011) we see that IVM is slightly different than the naturally occurring compound, an avermectin (Figure 3). The avermectin compound was first found in a soil sample from Japan as a natural fermentation product of the bacteria, *Streptomyces avermitilis.* Ivermectin was then developed by Merck & Co. and first introduced as an animal health drug in 1981. It

was not until 1988, under the name Mectizan®, that Merck & Co. released it for human use. It was donated as a part of MDA for onchocerciasis control in endemic areas. Ten years later it was registered for control of LF. It is the only macrocyclic lactone approved for human use and has been used to treat things from head lice to strongiloidiasis and scabies (Crump & Omura 2011, Tompkins et al 2010). Quite possibly one of the most important things about IVM is its safety for human use due to its specificity for invertebrates within the ecdysozoa.

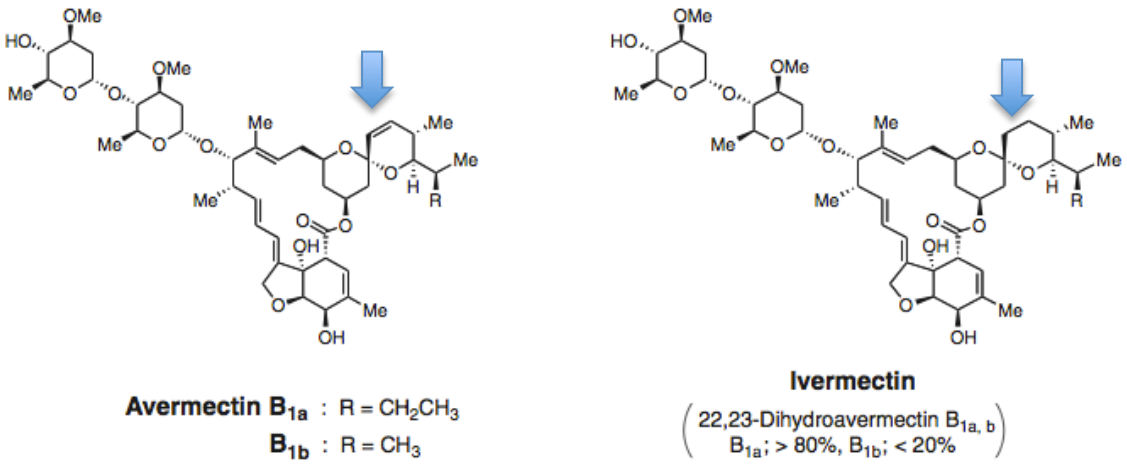

Figure 3: **Molecular structure of avermectin and corresponding ivermectin.** Ivermectin is made up of an 80:20 mixture of B1a and B1b avermectin and differs at one double bond (blue arrows).

Targets of Ivermectin

Originally gamma-aminobutyric acid (GABA) receptors in nematodes were thought to be the targets of IVM that caused impaired motility responses. GABA receptors have been shown to hinder nematode locomotion, discovered through the use of picrotoxin as a blocker of GABA receptors. Upon further investigation, it was noted that the concentrations of IVM required to elicit this response were well above clinically

relevant concentrations (Dent et al 1997, Wolstenholme & Rogers 2005). It was later discovered that glutamate-gated chloride channels (GluCls), on muscle and nerve cells, were the actual clinical receptors (McCavera et al 2007). GluCls were first described in locusts and have been shown to be similar across the protostome phyla. GluCls are pentameric structures of homo- or heteromeric origin. Each subunit is made up of an extracellular N- and C- terminus with four transmembrane domains (Figure 4) (Cully et al 1994). GluCls are closely related to GABA receptors and glycine receptors, which are characterized as a family called the cys-loop ligand gated ion family (Horoszok et al 2001, Wolstenholme & Rogers 2005). Binding of IVM, between M3 and M1, a different binding site from glutamate, to these channels results in a slow and irreversible hyperpolarization, which leads to varying degrees of paralysis (Dent et al 1997, Wolstenholme 2012). The size of this family is relatively variable among different species. The first cloned GluCls were from *Caenorhabditis elegans* and were expressed in *Xenopus* oocytes. *Caenorhabditis elegans* has six GluCl genes, of which avr-14, avr-15, glc-1 and glc-3 subunits form IVM-sensitive channels (Cully et al 1994, Dent et al 1997, Horoszok et al 2001, Vassilatis et al 1997). Mammals do not have any known GluCls, but have GABA and glycine receptors, which are sensitive to IVM. Most mammals have these additional receptors, but there is no real effect of IVM in mammals due to P-glycoproteins, a ABC-transporters, that can effectively keep the drug from crossing the blood brain barrier and accessing the receptors in the central nervous system (Wolstenholme & Rogers 2005). This results in a safe compound for human and animal use. Upon the completion of sequencing of the *B. malayi* genome it was found that the parasitic worm has fewer receptor genes than in *C. elegans* (Scott et al 2012). The only

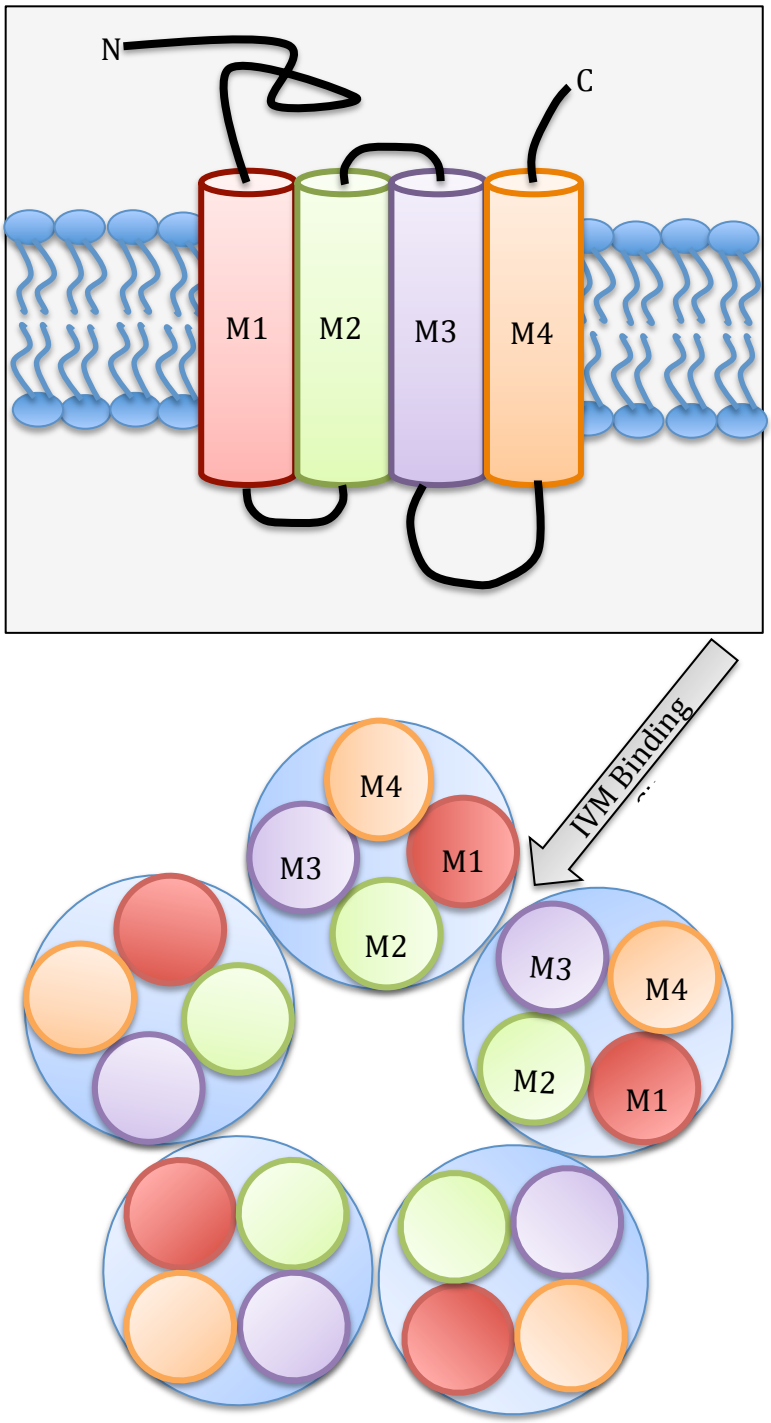

Figure 4: **Structure of GluCls.** The GluCls consist of four transmembrane domains (M1-M4) with an extracellular N-terminus and C-terminus. This figure was modified from Collingridge et al (2009) (top). Pentameric structure of a closed channel showing where the IVM binding site is located. This figure was modified from Wolstenholme (2012) (bottom).

IVM-sensitive channel is formed by avr-14 in *B. malayi* and has been shown to co-localize in an area where immunomodulatory proteins are secreted from mf (Moreno et al 2010, Williamson et al 2007, Wolstenholme & Rogers 2005). Direct evidence that the avr-14 from filarial nematodes can form IVM-sensitive channels has been obtained from the canine heartworm, *Dirofilaria immitis* (Yates & Wolstenholme 2004).

The Effects of Ivermectin on Filarial Nematodes

The effects of IVM on nematodes are species- and stage-dependent. As can be seen in a table modified from Tompkins et al (2010) it has a wide range of manifestations (Table 1). *In vitro,* the most noted effects of IVM on filarids are a reduction in motility in multiple life stages and sterility of adult females, however, these results are generally seen in response to IVM concentrations that exceed those used in therapy (Bennett et al 1988). *In vivo* infections in rodents revealed that IVM treatment with a standard dose of 0.15 mg/kg to 0.2 mg/kg causes a microfilaricidal effect in *Brugia spp., W. bancrofti, Onchochercha spp.* and *Dirofilaria immitis* and muscular passivity of mf in *Brugia spp*. In humans, treatment with IVM can almost completely clear mf from blood circulation within 36 hours of a single dose and this clearance has been long lasting (Moreno et al 2010, Ottesen et al 1990). In *Onchocerca* infections microfilaremia is reduced by 85-95% and in LF by 90% reported at one year post-treatment (Gonzalez et al 2012). While the mechanism of mf clearance from the blood is still unclear, it is postulated that long-lasting effects of IVM could be attributed to muscular paralysis of the vaginal muscles in the adult female, reducing mf output, or even inability of the adult male to travel to fertilize the oocytes in the female due to whole-body paralysis (Tompkins et al 2010).

Another proposed mechanism of clearance is via paralysis of the excretory/secretory pore, resulting in a decrease of immunomodulatory protein secretion. This mechanism would allow for the host's immune system to recognize the infection and potentially eliminate it (Bennett et al 1988, Moreno et al 2010). The paralysis of helminth musculature is elicited via binding of IVM to its targets.

Table1: ***In vitro* and *in vivo* effects of IVM on multiple helminth species.** *In vitro* effects of IVM on helminths from multiple studies (top); *In vivo* (bottom).

In vitro	
Filarioid Species	Phenotype
Brugia malayi	Impaired adult, mf, and L3 motility Death of adults and L3 Reduced mf output Cuticular damage in L3
Wuchereria bancrofti	Inhibited molting in L3
Onchocerca volvulus	Reduced motility in mf and adult males
Onchocerca lienalis	Reduced motility in mf Killing of mf
Monanema martini	Impaired embryogenesis
In vivo	
Brugia malayi and *Brugia pahangi*	Killing of mf [a,b] Altered embryo morphology [b] Muscular passivity in mf [b] Impaired mf exsheathing [b]
Wuchereria bancrofti	Killing of mf [a] Reduced mf output [a] Potential sterilization of females a
Onchocerca volvulus, lienalis, cervicalis	Killing of mf [a,b,c] Impaired embryogenesis
Dirofilaria immitis	Killing of mf *in utero* [d] Killing of adults [d] Impaired motility of adults [d]
Monanema martini	Impaired embryogenesis [b]

[a] Human host
[b] Rodent host
[c] Equine host
[d] Canine host

Ivermectin Effects in Humans with Lymphatic Filariasis

Within 36 hours of administering a single dose of IVM there is a significant decrease in mf in the blood. By two weeks post-treatment, the mf are completely cleared from circulation. By one year post-treatment subjects had resumed microfilaremia (Brown et al 2000). The absence of mf can be sustained for at least six months (Ottesen et al 1990). Due to high lipid solubility of the drug, IVM is widely distributed in the body, which results in a plasma half-life of about half a day to a day (Gonzalez et al 2012, Merck & Co. 2002). Due to the absence of GluCls in mammals, adverse events are relatively unrelated to toxicity of the drug itself. Most side effects are actually attributed to the human immune response to dying worms and their endosymbiont, *Wolbachia* (Arndts et al 2012).

Human Immune Responses to Helminths

Human immune responses to helminth infections are species- and stage-dependent. Unfortunately, the immune response to helminths in a human infection is very difficult to study and most of the experiments that have been performed on immune mechanisms rely on animal models or *in vitro* assays with human components.

Before discussing the cytokine responses related to LF infections, a basic overview of some of the effector cells involved in the pathology is essential. Granulocytes, such as eosinophils and neutrophils, play a large role in responses to helminths. They produce chemicals, called alarmins, which aid in fighting invasion. Eosinophils are characteristic of helminth infections. In a healthy individual they make up around 2-5% of white blood cells in the peripheral blood, whereas in an infected

individual they can comprise 40% of the cells in the blood. *In vitro* experiments have shown that *Brugia spp*. mf are killed in response to granular proteins released from eosinophils. In LF, eosinophils have been shown to be required for killing of primary infections with L3s. Another key player are the neutrophils. They are often the first cells to respond to inflammation and they can release granules into the environment to fight invaders. Primary granules consist of myeloperoxidase acid hydrolases, lysozyme, defensins, and serine proteases, while secondary granules consist of lactoferrin and lysozyme. Other effector cells, such as basophils and mast cells have not been studied due to their supposed lack of necessity in filarial infections (Cadman & Lawrence 2010).

Immune responses to helminth infections are stage-specific and dependent on the host's age and history of infection. Gastrointestinal helminth infections have generally been classified as Th2 polarized where eosinophilia, mastocytosis, and high levels of circulating IgE are noted. These responses are characterized by increased production of inflammatory cytokines such as IL-4, IL-5, IL-9, and IL-13 and a decrease in regulatory components such as IL-10, TGF-β, and regulatory T cells (Tregs) (Bourke et al 2011, Maizels & Yazdanbakhsh 2003). However, infections with filarial nematodes are generally not this simple and the immune response to filarial helminths is much more variable. I will focus on the immune response to filarial infections involved in LF. Most studies have been performed on the adult and mf stages of the filarids that cause LF, however, the first line of defense is the skin in relation to the infective stage of the parasite, L3 larvae. Here L3s interact with Langerhans cells (LC), but the effects of L3s on the activation of LCs seems to be nonexistent *in vitro*, suggesting that LCs do not play a role in antigen presentation in this model, or that L3s have developed an

immunomodulatory mechanism for entrance into the body (Boyd et al 2013). *In vivo* studies in humans on L3's are difficult to execute due to the difficulty of pinpointing when infections first occurs. Most *in vivo* experiments are performed in animal models and display different immune responses. In most susceptible animal models a non-polarized immune response is noted, while in resistant murine models the response is Th2 polarized. When live *B. malayi* L3s are exposed to naïve human peripheral blood mononuclear cells (PBMC) *in vitro*, surprisingly, a strong Th1 response ensues and could possibly be the cause of the symptoms associated with acute LF (Babu & Nutman 2003). Acute infections have been associated with lymphocyte proliferation, mixed cytokine production (IL-2, IFN-γ, IL-5, TNF-α, and IL-8), eosinophilia, increased IgE and lower levels of IgG4 (Babu & Nutman 2003, Nutman & Kumaraswami 2001). A Th1 response is also seen in normal individuals from non-endemic areas and is hypothesized to be the reason they remain uninfected (Babu & Nutman 2003).

As infection progresses to patency in laboratory models, the immune response is altered. Decreased lymphocyte production, IL-2, IFN-γ, and an increase in IgG4 and IL-10 are noted. It is proposed that the increase in IgG4 provides protection against immunopathology for the host and parasite against the effects of IgE (Arndts et al 2012). These individuals usually have adult worms in the lymphatics and mf circulating in the blood and are misleading due to a relatively silent, but active infection (Babu & Nutman 2003). These effects have been shown to be dependent on parasite burden and the length of infection (Nutman & Kumaraswami 2001). In general, asymptomatic infections are Th2 mediated and more permissive, while chronic infections are related to increased inflammatory responses and elephantiasis (Babu et al 2009). This typical response is not

evident, however, in cases of tropical pulmonary eosinophilia (TPE). TPE results when mf are trapped and die in the lungs, resulting in a drastic inflammatory reaction (Cadman & Lawrence 2010, Nutman & Kumaraswami 2001). Unfortunately, despite the best attempts of the host's immune adaptation to stave off an infection, helminths have developed their own mechanisms of evading detection and neutralization.

Immunomodulation by Filarial Nematodes

Parasitic helminths have developed ways to evade immune recognition. The scientific community is aware of some of these mechanisms, but there is little that is definitively known about how helminths mediate these responses. There are many reports implicating interference with antigen presentation, reactive oxygen species generation, and even effector cell recruitment (Maizels & Yazdanbakhsh 2003, Schroeder et al 2012). There seems to be some controversy as to which stage of the parasite has the most immunomodulatory functionality. Some claim the ability of parasites to evade and modulate immune recognition seems to increase as they mature (Nutman & Kumaraswami 2001). Others have found that the more immature form to reside in a human, the mf, actually produce the most immunomodulatory proteins when compared to the adults (Bennuru et al 2009). Whichever stage dominates immune evasion, most researchers are agreed that the immunomodulatory factors are mainly secreted from the excretory/secretory pore (Bennuru et al 2009, Li et al 2012, Maizels & Yazdanbakhsh 2003, Moreno et al 2010). Many of the known immune modulators are proteins, such as cysteine proteinase inhibitors and serine protease inhibitors that interfere with antigen presentations, cytokine mimics of TGF-β that can decrease cell activation, and

macrophage migration inhibitory factor homologs that interfere with recruitment of effector cells (Bennuru et al 2009, Schroeder et al 2012). *Brugia malayi* adults and mf displayed higher levels of mRNA for adhesion molecules PECAM-1 and VE-cadherin along with Junctional Adhesion Molecule C (JAM-C) suggesting a stronger binding that could interfere with the rolling of cells on the vascular endothelium. Even the *Wolbachia* endosymbiont, required for growth of *B. malayi*, was shown to inhibit recruitment of macrophages and monocytes through the action of host adhesion molecules ICAM-1 and VCAM-1 (Schroeder et al 2012). These factors can form a tight barrier in which some of the body's main effectors cannot get through.

It is important to remember that the immune heterogeneity of the host and filarial parasite develop based on the environment in which the two species interact. There is great variability in genes expressed, immune modulation, and immune reactivity between life stages and even amongst different biological replicates and different laboratory models (Bourke et al 2011). The way in which these entities react to each other is determined in the host at a very young age and is modeled throughout the lifetime of the host and parasite.

Conclusion

Lymphatic filariasis is an extremely debilitating disease that affects a large portion of the population in developing countries. The causative agents of LF are *Wuchereria bancrofti, Brugia malay,* and *B. timori* and can cause extreme morbidity and pose a threat in everyday life. Control of these filarial nematodes is reliant on programs implementing mass drug administration in an attempt to decrease transmission of the

disease. Mass drug administration relies on a yearly treatment with IVM or DEC paired with ALB. Ivermectin alone is considered a wonder drug for its specificity for the ecdysozoa and for its safety in humans and animals. While much is left to be discovered as to the mode of action of ivermectin in LF, a recent finding by Moreno et al (2010) has given rise to the idea that IVM acts in conjunction with the host's immune system to eliminate infection. These findings have yet to be confirmed in an *in vivo* model, but could have great implications in understanding the mode of action of IVM to decrease transmission of LF in the developing world.

CHAPTER 2

INTRODUCTION

Lymphatic filariasis is a disease associated with high levels of morbidity, disfigurement, and social stigmas in those who have been infected. The World Health Organization has estimated that 120 million people are currently infected with at least one of the causative agents of LF, a filarial nematode. *Wuchereria bancrofti* and *Brugia malayi* are responsible for almost 100% of diagnosed cases in 73 countries worldwide, with 1.4 billion at risk for infection. In 2000, the WHO developed the GPELF with two main goals in mind: disrupt transmission through MDA and treat the symptoms of those already affected by the disease (WHO 2011).

Mass drug administration is currently a single dose two-drug regimen of ALB (400 mg) paired with DEC (6 mg/kg) in onchocerciasis non-endemic areas, or with IVM (0.2 mg/kg) where onchocerciasis is prevalent. It is recommended that treatment be continued annually for four to six years to fully reduce transmission. While DEC was the first drug used to treat these diseases, the discovery of IVM revealed a faster, safer, more effective drug that can be used in areas where DEC is contraindicated (Gonzalez Canga et al 2008, Horton et al 2000). Ivermectin is a derivative of a naturally produced chemical and is the only macrocyclic lactone that is approved for human use. Since IVM's discovery in 1970, its efficacy has been demonstrated for multiple ailments (Crump & Omura 2011, Tompkins et al 2010). With a wide array of uses, resistance to IVM and

related drugs has arisen in parasites of livestock and companion animals, including canine heartworm, and has made it imperative to understand the mode of action of this drug. The main targets of IVM in filarial parasites are glutamate-gated chloride channels, which were first described in insects (Wolstenholme 2012). Binding of IVM to the GluCls hyperpolarizes the muscle and results in paralysis. In the gastrointestinal nematodes, this leads to paralysis of the pharynx and subsequently starvation and death, or to paralysis of the body wall musculature, resulting in expulsion from the host (Tompkins et al 2010, Wolstenholme 2012).

Brugia malayi adults reside in the lymphatic system, and the mf are in the peripheral blood and the arterioles of the lungs. They are exposed to different environments than those seen by the G.I. nematodes (Hawking & Gammage 1968). One major difference from the G.I. nematodes is that filarial nematodes are thought to get their nutrients through their cuticle instead of pharyngeal pumping, due to having an atrophied gut. This indicates that starvation, due to paralysis of the pharynx, is probably not the mode of killing by IVM in these nematodes (Tompkins et al 2010). Despite these discrepancies, treatment with a single dose of IVM causes mf to disappear within 36 hours and they do not return for up to six months (Moreno et al 2010, Ottesen et al 1990). There is currently no evidence to explain how IVM elicits this effect nor where the mf go.

In an untreated infection, filarial nematodes are often able to escape recognition by the host immune system. They have been known to live in their hosts for up to 10 years. Their ability to live in a host for long periods of time, unrecognized by the immune system, suggests that they have methods of immunomodulation. This

immunomodulation has been attributed to secretion of specific proteins from the excretory/secretory apparatus. Not all of the proteins secreted from the ES pore are immunomodulatory, but proteins such as migration inhibitory factor (MIF-1) homolog, cystatin-type cysteine proteinase inhibitor (CIP-2), and ES-62 have been identified as potential immunomodulators and are secreted by various life stages of *B. malayi* (Bennuru et al 2009, Choi et al 2011, Li et al 2012, Moreno & Geary 2008). It has recently been demonstrated in *B. mala*yi mf, that the target of IVM, avr-14, localizes to the musculature surrounding the ES pore, and thus treatment of these mf with IVM decreases secretion of these immunomodulatory proteins (Moreno et al 2010). This observation, paired with the fact that it takes higher levels of IVM *in vitro* to achieve paralysis than to achieve mf clearance *in vivo*, suggests that IVM could be acting in conjunction with the host's immune system to clear the mf from circulation, thus reducing transmission (Tompkins et al 2010). Recent research from our lab, performed on a closely related filarial species, the canine heartowrm, *Dirofilaria immitis*, has demonstrated a role for the immune system in a possible mode of action for IVM. Canine peripheral blood mononuclear cells (PBMCs) and neutrophils have shown a drug-dependent attachment to *D. immitis* mf in *in vitro* assays (Figure 5)(Vatta, A., personal communication).

To our knowledge, no one has demonstrated that the binding of IVM to its targets increases host immune recognition in *B. malayi* or has evaluated the transcriptome of *B. malayi* mf, treated *in vivo*, with IVM. In this study, we assess the ability of IVM to paralyze *B. malayi* mf. We also assess the ability of human neutrophils to bind to mf

when treated with and without varying concentrations of IVM. Finally, through RNAseq analysis, we evaluate the effects of IVM on transcription in an *in vivo* model. With the potential of increasing resistance to a 'wonder drug' it is imperative to understand the mechanism of action for future drug screening and the preparation of resistance in human associated filarial parasites.

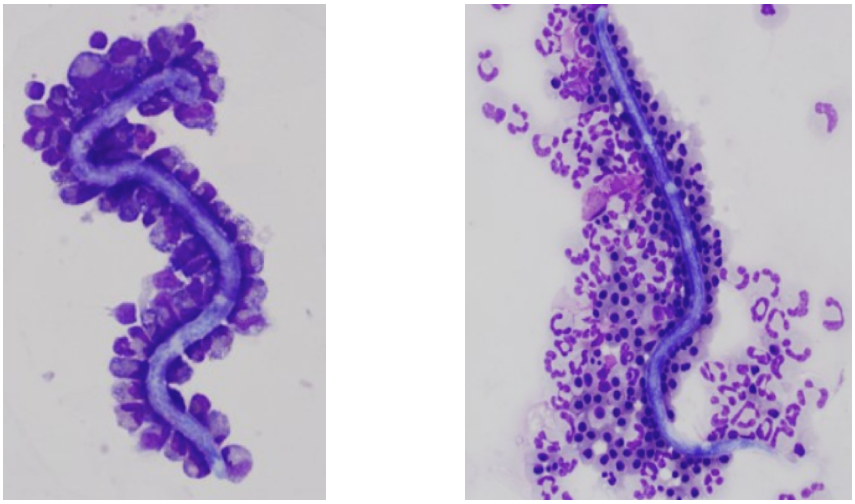

Figure 5: **Drug-dependent immune cell attachment in response to *D. immitis* mf.** PBMCs attached to a canine heartworm mf in a drug dependent manner (left). Neutrophils attached to a canine heartworm mf in a drug dependent manner (right). Pictures by Dr. Melinda Camus.

CHAPTER 3

MATERIALS AND METHODS

Ivermectin Preparation

For *in vitro* assays a 10 μM stock solution of IVM (Sigma, St. Louis, MO) was made by dissolving 8.75 mg of IVM into 1ml of dimethylsulfoxide (DMSO; Sigma). Serial dilutions were made to achieve 0.001 μM to 1mM IVM in DMSO. These were each diluted in RPMI-1640 (Life Technologies, Grand Island, NY) to achieve final concentrations of 0.02 nM to 20 μM IVM in 2% DMSO (v/v). Concentrations of IVM in a 96-well plate (Corning, Corning, NY) assay ranged from 0.01 nM to 10μM and the final concentration of DMSO was 1% (v/v).

For animal treatment, a 20 mg/ml solution was made by dissolving IVM in DMSO. The solution was then diluted to 0.2 mg/ml and sterilized by filtration through a 0.2 μm syringe filter (Corning).

Animal Infection and Treatment

Mongolian gerbils, *Meriones unguiculatis* (Filariasis Research Reagent Resource Center; FR3, Athens, GA) were injected intraperitoneally with 300 to 400 *B. malayi* infective third stage larvae (iL3; FR3) that had been extracted from mosquitoes (*Aedes aegypti,* black-eyed Liverpool strain; FR3). The infection was allowed to progress for at least three months until patency was achieved. The gerbils were randomly divided into

treatment groups and were injected subcutaneously with the vehicle control, DMSO, or 0.2 mg/kg IVM.

Media Preparation

RPMI-1640 was supplemented with penicillin-streptomycin (10,000 U/ml; Life Technologies) for a concentration of 100 U/ml, and gentamicin (10 mg/ml; Sigma, St. Louis, MO) for a concentration of 0.1 mg/ml. This was aliquoted into 50 ml Falcon tubes (Becton Dickinson, Franklin Lakes, NJ) and stored at 4°C. Before each use, the pH of the solution was tested to ensure a range from 7.0 to 7.5, the physiological pH needed to maintain healthy *B. malayi*.

Parasite Purification

For all assays, *B. malayi* mf from gerbil peritoneal lavage (FR3) were filtered through a 10 μm mesh to exclude contamination with larger particles. They were pelleted by centrifuging at 3000 rpm for five minutes and washed with RPMI-1640. Aliquots were filtered again using a PD-10 desalting column (GE Healthcare, Buckinghamshire, UK) according to the PD-10 Product Gravity Protocol and using RPMI-1640 containing antibiotics as the equilibration buffer. The same column was used multiple times for the same sample of peritoneal fluid until all of the fluid had been filtered. The eluate was examined under a microscope to ensure mf presence and viability. Viable mf were maintained in a tissue culture flask with vented cap (Corning) in an incubator at 37 °C and 5 % CO_2 for use within the next 24 hours.

For RNA extraction, adult *B. malayi,* removed from gerbils treated with two to three doses of the vehicle control, DMSO, or 0.2 mg/kg IVM, were separated based on sex, washed three times with phosphate buffered saline (PBS; Sigma), and aliquoted into 2 ml cryogenic vials with 10 to 20 adult worms per vial. Each vial underwent flash freezing with dry ice submerged in ethanol and was stored at -80°C.

Brugia malayi mf, removed from gerbils treated with two to three doses of the vehicle control, DMSO, or 0.2 mg/kg IVM, were centrifuged for five minutes at 3000 rpm and washed three times with PBS. They were resuspended in 2.5 ml of PBS and 500 µl aliquots were flash frozen with dry ice, submerged in ethanol, and stored at -80°C.

Motility Assay

Approximately 50 *B. malayi* mf were pipetted into each well, of a 96-well plate, containing RPMI-1640 with antibiotics. Ivermectin was added to designated wells for final concentrations of 0.01 nM, 0.1 nM, 0.001µM, 0.01µM, 0.1 µM, 1 µM, 2.5 µM, 5 µM, and 10 µM. The 96-well plate was then incubated at 37 °C and 5 % CO_2 for 16 to 24 hours. Each well was visualized on an inverted microscope at 20X magnification. Approximately 50 mf from each well were scored using a method modified from Khunkitti et al, (2000) and Zaridah et al (2001). The scoring was as follows:

0 -- no movement for more than 10 seconds

1 – less active; ≤ 5 head or tail twitches in 10 seconds

2 – moderately active; slightly slower thrashing motions

3 – highly active; normal thrashing motions

Neutrophil Attachment Assay

Approximately 50 *B. malayi* mf were pipetted into each well of a 96-well plate containing RPMI-1640 with antibiotics. Normal human serum was added to half of the wells to achieve a final concentration of 5% v/v. Human neutrophils were extracted and purified as described in a protocol by Pang et al (2013). Briefly, red blood cells were removed from whole blood via Dextran sedimentation. White blood cells were washed in PBS, free of calcium and magnesium, subjected to a 5-phase Percoll gradient, and the layers containing neutrophils were washed with PBS. Neutrophils were stored in a 1:1 mixture of serum and RPMI-1640 until needed. The neutrophils were washed upon use with RPMI-1640 and added to designated wells to achieve three neutrophil-to-worm ratios: 300:1, 1000:1, 3000:1. Ivermectin was added to designated wells for final concentrations of 0.01 μM, 0.1 μM, 1 μM and 10 μM. The plates were incubated at 37 °C and 5 % CO_2 for 16 to 24 hours. Each well was visualized on an inverted microscope at 40X magnification. Approximately 50 mf were scored for neutrophil attachment. Attachment was defined as any mf that had at least one neutrophil attached, either directly touching or indirectly attached by extracellular DNA.

Neutrophil Activation Assay

On Day One, 50 *B. malayi* mf were added to designated wells with RPMI-1640 with or without 1 μM IVM. They were incubated overnight at 37°C with 5% CO_2. On Day Two, 5% (v/v) autologous human serum was added to each well. Neutrophils were added to designated wells at a neutrophil-to-worm ratio of 3000:1. Ivermectin was added again to the same wells as Day One to maintain a 1 μM solution. Phorbol myristate

acetate (PMA), 100 nM, was used as a positive control and RPMI-1640 was used as a negative control. The plate was incubated for 4 hours at 37°C with 5% CO_2. SYTOX® Orange (Life Technologies; 5mM), diluted to 2.5 μM, and Hoechst DNA dye were added to every well and allowed to incubate for 20 minutes. Each well was visualized using EVOS® FL Cell Imaging System (Life Technologies). Each well was imaged at three random locations and the fluorescence of wells was compared.

RNA Extraction

All surfaces and equipment used for RNA extraction were treated with RNase AWAY™ (Life Technologies). All tubes used in RNA extraction were diethylpyrocarbonate (DEPC; Sigma) treated. All water used in the process was labeled as nuclease free.

RNA extraction was performed on flash frozen *B. malayi* adults and mf, exposed *in vivo* to DMSO or IVM. Sample preparation was performed using a modified TRIzol® Reagent (Life Technologies) protocol. Briefly, 3 ml of TRIzol® was added to one sample of frozen *B. malayi* adult or mf and homogenized using a mortar and pestle or a tissue homogenizer. They were then aliquoted three times into 1 ml tubes and centrifuged for 10 minutes at 12,000 x g at 4°C to pellet the solid material. After a five-minute incubation period at room temperature, the supernatant was added to a new tube and mixed with 0.2 ml of chloroform (Sigma). After a three-minute incubation at room temperature, the samples were centrifuged again for 15 minutes under the same specifications. The aqueous layer was added to an RNA Clean and Concentrator ™-25 spin column (Zymo Research, Irvine, CA) and the procedure was completed as per

product instructions. Eluted RNA samples were analyzed on a NanoDrop 2000 Spectrophotometer (Thermo Fisher Scientific, Pittsburgh, PA) to determine their concentration and to measure the 260/280 absorbance ratio. Samples with a 260/280 ratio above 1.75 were sent to the Georgia Genomics Facility (GGF; Athens, GA) for integrity analysis on an Agilent 2100 Bioanalyzer (Agilent Technologies, Santa Clara, CA) using an RNA 6000 nano chip. Samples with an RNA Integrity Number (RIN) of ≥ 8 were used for RNAseq.

RNAseq

Good quality total RNA (1-10 μg) was sent to GGF for preparation for sequencing. Sample preparation was performed using TruSeq RNA Sample Preparation Kit (Illumina, San Diego, CA). The prepared samples were then sent for sequencing on the Illumina HiSeq 2000 v3 using PE50 as the run type. The output from these runs was submitted to GGF for bioinformatics analysis.

RNAseq Analysis of Results

RNAseq analysis was performed by GGF. TopHat v 2.0 (Center for Bioinformatics and Computational Biology, CBCB; College Park, MD) was used to align the transcripts to a reference genome (Scott & Ghedin 2009). Transcripts assembly, transcriptome assembly, and gene and transcript expression were calculated using Cufflinks (CBCB). The significantly-differentially expressed transcripts were compared to the *B. malayi* genome using the Basic Local Alignment Search Tool (BLAST). Any identical contigs were aligned with Geneious v 6.1 (Biomatters, San Francisco, CA)

default settings. Contigs with identity of 95% or higher were considered the same and a consensus sequence was generated. These consensus sequences and other redundant significant transcripts were aligned to evaluate if these were encoding the same gene, splice variants, or unique transcripts. The top 10 up- and down- regulated transcripts were studied further in qPCR experiments.

Primer Design

Primers for RT-PCR and qRT-PCR were designed using the Eurofins MWG Operon Primer Design Tool with the default settings. Primers were provided by Eurofin MWG Operon (Huntsville, AL).

Reverse Transcription of RNA to cDNA

RNA, with an RIN of ≥ 7, was reversed transcribed to cDNA using qScript™ cDNA Synthesis Kit (Quanta Bioscience, Gaithersburg, MD). The reactions were combined in 500 µl microcentrifuge tubes as follows:

RNA (1µg to 10 pg total RNA)	1 µl
Nuclease-free water	14 µl
qScript Reaction Mix (5X)	4 µl
qScript RT (25 U/ml)	1 µl
Total	20 µl

Reactions were run on a T100™ Thermal Cycler (Bio Rad, Hercules, CA) with the following program:

1. 22°C, 5min

2. 42°C, 30 min
3. 85°C, 5 min
4. 4°C, hold

Gel Electrophoresis

Samples were run on 2% (w/v) agarose gel made by dissolving Certified™ Molecular Biology Agarose (Bio Rad) in 1 x TAE buffer (National Diagnostics, Atlanta, GA). The solution was microwaved until agarose granules dissolved and then allowed to cool on the bench for 15 minutes. Ethidium bromide (Sigma) was added to the cooled solution to achieve a final concentration of 0.05 μg/ml. After swirling, the solution was poured into a gel tray and the appropriate sized comb was added. The gel was allowed to solidify and was then added to an electrophoresis tank filled with 1 x TAE buffer. Blue/Orange Loading Dye 6x (Promega) was added as needed to samples. Approximately 10 μl of each sample and a 100bp ladder (Promega) were pipetted into the wells. Full-sized gels were run for one hour at 100 volts. Half-sized gels were run for 30 minutes at 100 volts. Upon completion, gels were visualized under a transilluminator (Syngene, Frederick, MD) using GeneSnap software v 7.12.06.

RT-PCR

PCR was performed on cDNA using GoTaq® Hot Start Green Master Mix (Promega, Madison, WI). Components were added to a 0.2 ml thin-walled PCR tube as follows:

GoTaq® Hot Start Green Master Mix, 2X	25μl

Upstream primer, 10μM	1 μl
Downstream primer, 10μM	1 μl
DNA template (<250 ng)	1 μl
Nuclease-Free Water	22 μl
Total	50 μl

Reactions were run on a T100™ Thermal Cycler (Bio Rad, Hercules, CA) with the following program:

1. Initial Denaturation	95°C	5 min
2. Denaturation	95°C	30s
3. Annealing	variable	30s
4. Extension	72°C	1 min
5. Go to Step 2, 34 times		
6. Final Extension	72°C	5 min
7. Hold	4°C	

The annealing temperatures were set to be 3°C below the lowest primer Tm. The products were then run on a 2% agarose gel to ensure proliferation of only one product. Samples that resulted in one band of the correct size were subjected to qPCR.

qPCR

Quantitative PCR was performed on cDNA using PerfeCTa™ SYBR® Green Fastmix™, Low ROX™ (Quanta Biosciences). Reactions were set up is 0.2 ml thin walled PCR strips and flat top caps (Corning), as follows:

PerfeCTa SYBR Green FastMix, Low ROX (2X)	10 μl

Forward Primer (10 μM)	1 μl
Reverse Primer (10 μM)	1 μl
Nuclease-free water	7 μl
Template	1 μl
Total	20 μl

Each reaction was run on an Mx3000P Thermocycler (Stratagene,) using Mx3000 software v 4.01 for data collection. The program was as follows:

1. 95° C for 10 mins
2. 95° C for 30 secs
3. variable for 30 secs
4. 72° C for 1 min
5. Go to step 2, 40 times
6. 95° C for 1 min
7. 55° C for 30 secs
8. 95° C for 30 secs

CHAPTER 4

RESULTS

Motility Assay

To identify the concentration of IVM required to paralyze *B. malayi* mf *in vitro* motility assays were performed on 50 mf in triplicate. Approximately 90% of the mf remained motile in media treated with IVM up to 1µM (Figure 6). The results indicated that the point where 50% of the mf were paralyzed, the EC_{50}, was around 3 – 4 µM and 10 µM was sufficient to completely paralyze 100% of the mf *in vitro*.

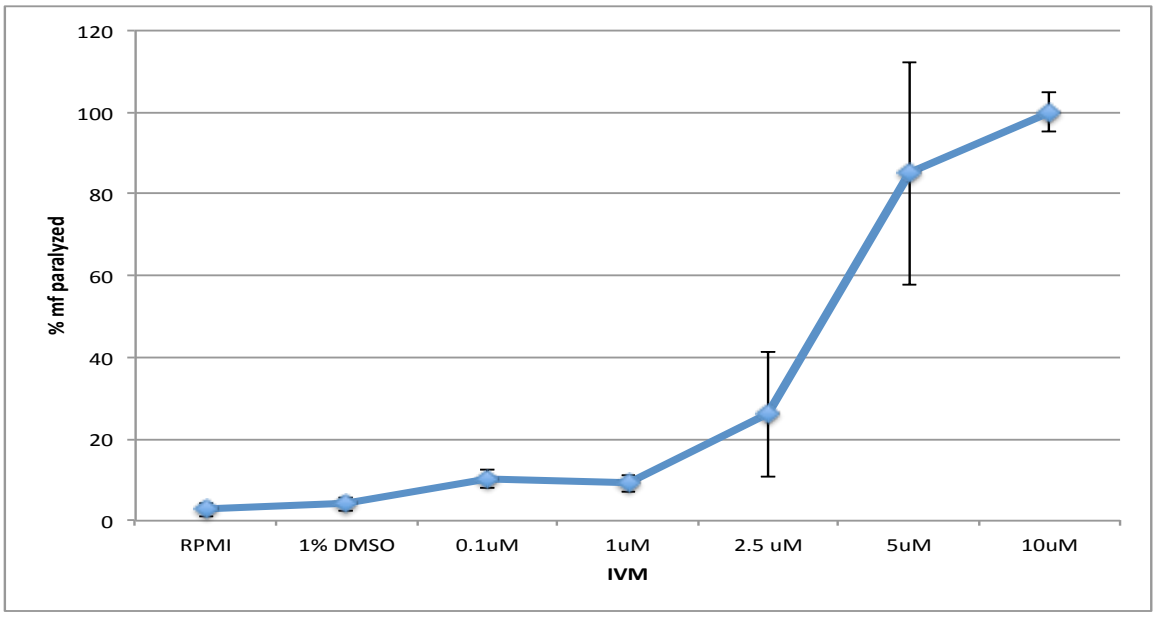

Figure 6: **Paralysis of *B. malayi* mf *in vitro* when exposed to differing concentrations of IVM.** Approximately 50 mf were exposed to IVM ranging from 0.01 nM to 10 µM. The assay incubated for 16 hours and each mf was scored (0-3) based on motility as described in the methods section. Scores of 0 and 1 make up the 'Paralyzed/Dead' and are plotted in this graph. This assay was performed in triplicate and repeated for a total of four independent experiments. Error bars are representative of the S.E.

Neutrophil Attachment Assay

The concentrations of IVM required to paralyze mf *in vitro* are much higher than those they are exposed to in drug administration programs, which suggests that a direct effect of the drug may not be sufficient to explain the rapid clearance of the mf observed *in vivo*. To assess the ability of IVM to prevent mf immune evasion, 50 *B. malayi* mf were exposed to varying levels of normal human neutrophils, autologous human serum, and IVM *in vitro* (Figure 7). Wells containing no neutrophils served as a control to ensure the health of the mf independent of the neutrophils, and thus were not scored for attachment.

		Neutrophil : Mf											
	IVM (uM)	No Neutrophils			300 : 1			1000 : 1			3000 : 1		
No Serum	0												
	0.1												
	1												
	10												
5% Normal Human Serum	0												
	0.1												
	1												
	10												

Figure 7: **Standard 96-well plate layout for Neutrophil Attachment Assay**. Approximately 50 mf were exposed to varying ratios of normal human neutrophils (300:1, 1000:1, or 3000:1), medium, medium supplemented with 5% autologous human serum, and IVM (0.1 µM to 10 uM). After a 16-hours incubation period each mf was scored (yes or no) for neutrophil attachment.

There were three types of neutrophil attachment observed in the wells. Direct attachment was scored if at least one neutrophil could be seen directly attached to the mf (Figure 8 A). Indirect attachment was considered when the neutrophils were not necessarily directly attached, but had more of a web-like appearance. Indirect attachment was identified by visualizing neutrophils moving in synchronization with the mf without actually having direct contact (Figure 8 B). The third condition was termed a neutrophil mass in which multiple mf were engulfed in a large mass of neutrophils (Figure 8 C). If any of these attachment types were observed the mf was scored as positive for attachment.

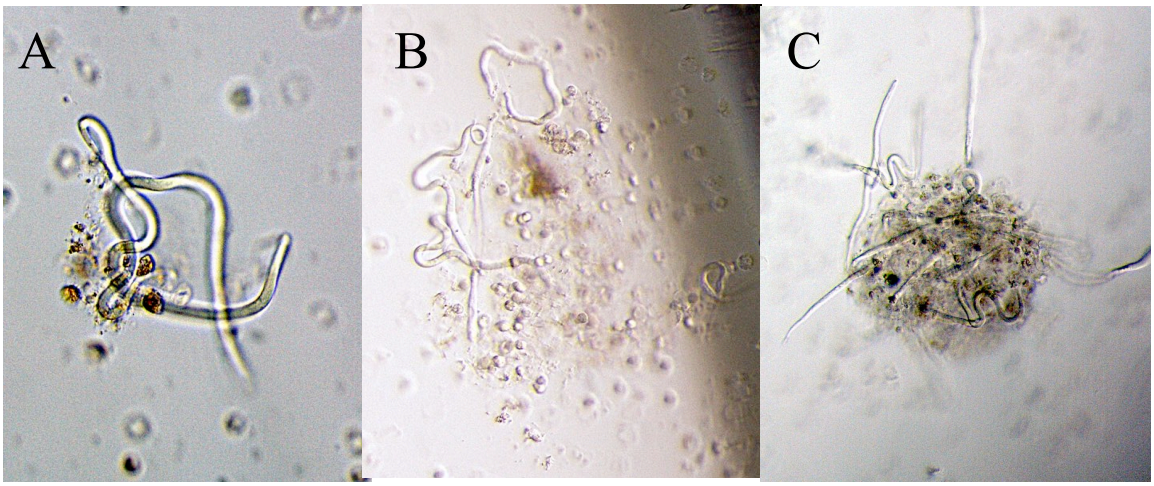

Figure 8: **Types of neutrophil attachment *in vitro* to *B. malayi* mf**. A) Direct attachment; B) Indirect attachment; C) Neutrophil mass.

The higher the neutrophil-to-worm ratio, the more attachment of neutrophils to mf was observed independently of serum (Figure 9 A and B). Ivermectin seemed to have no effect on the level of neutrophil attachment under any of the tested concentrations. The addition of serum resulted in a decrease in the level of attachment for all neutrophil-to-worm ratios and for all IVM concentrations (Figure 9 B). In the group 300:1 neutrophils-to-mf, the addition of serum decreased neutrophil attachment by 25-32%. In

the 1000:1 group the attachment was decreased by 34-43%. In the 3000:1 group attachment was decreased by 39-46%. In the absence of serum all mf exposed to 10 µM IVM were paralyzed and could not effectively be scored for attachment (Figure 9A). However, in the presence of serum all mf exposed to 10 µM IVM were still active and available for scoring.

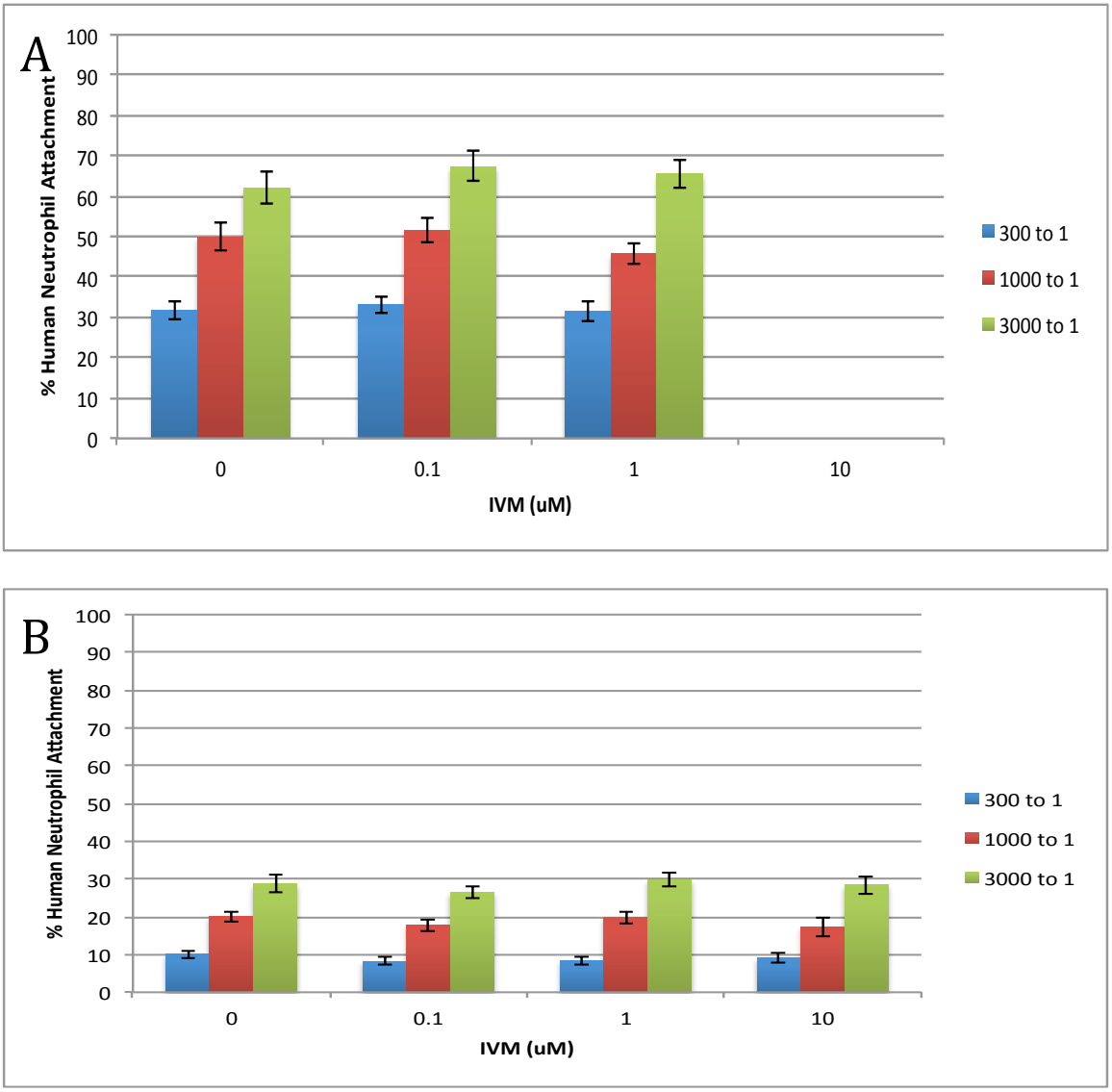

Figure 9: **Neutrophil attachment to *B. malayi* mf *in vitro***. A) Neutrophil attachment to mf in the absence of serum. B) Neutrophil attachment in the presence of 5% autologus human serum. The colored bars represent neutrophil attachment with different neutrophil-to-mf ratios: blue (300:1), red (1000:1), and green (3000:1). Each condition was performed in triplicate and repeated for a total of five individual experiments. Error bars are representative of S.E

Neutrophil Activation Assay

Extracellular DNA from neutrophils can be used as a measure of neutrophil activation. In order to assess neutrophil activation, fluorescence of normal human neutrophils co-incubated with autologous serum and with or without mf and IVM was observed. A membrane-impermeable DNA dye was added 30 minutes before visualization. Three time points were observed post-neutrophil addition (2 hrs, 4 hrs, and 21 hrs) to determine the best time for observation. Zero hours was considered the time point at which the neutrophils were added. At two hours there were no observable differences in fluorescence amongst the treatment groups, even in the positive control wells treated with 100 nM PMA (Figure 10). At four hours no visual differences were seen in neutrophil activation between the negative control and the mf with 1 μM IVM wells. There was a slight decrease in fluorescence observed in the wells containing mf and no IVM when compared to the negative control well and 1 μM IVM well containing mf. The PMA-treated wells had significantly more activation overall upon visual inspection (Figure 11). At 21 hrs the wells containing mf had more fluorescence than the control wells, and those with IVM show higher fluorescence than those without drug (Figure 12). Inspection of the positive control wells in visual light revealed a noticeable reduction in the total number of neutrophils when compared to the 2 hr and 4 hr time points and for this reason it was not used in the assessment. There was no drug-dependence noted in relation to neutrophil attachment to *B. malayi* mf, however neutrophil activation seemed to be greater, at 4 hours, in the wells containing mf and 1 μM IVM possibly indicating that this may be a more sensitive test to determine the effect of IVM on neutrophils in relation to mf.

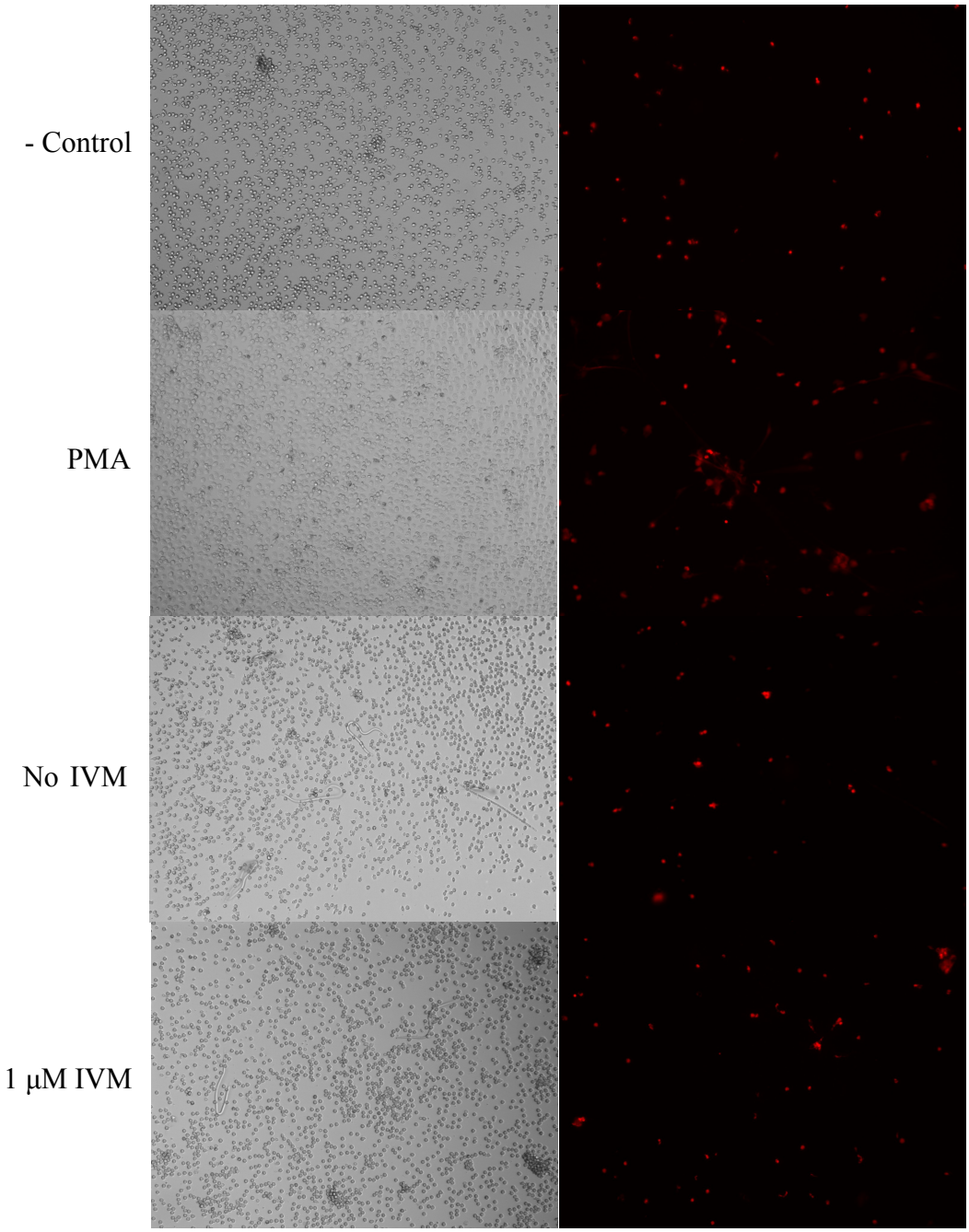

Figure 10: **Normal human neutrophil activation 2-hrs after the addition of neutrophils**. Human neutrophils were exposed to 5% autologous serum and RPMI 1640, 100 nM PMA, *B. malayi* mf, or *B. malayi* mf and 1 μM IVM. The controls wells have no mf while the two IVM wells both have mf. Each condition was performed in triplicate, with each well being imaged at three random locations. Each image is representative of three independent assays.

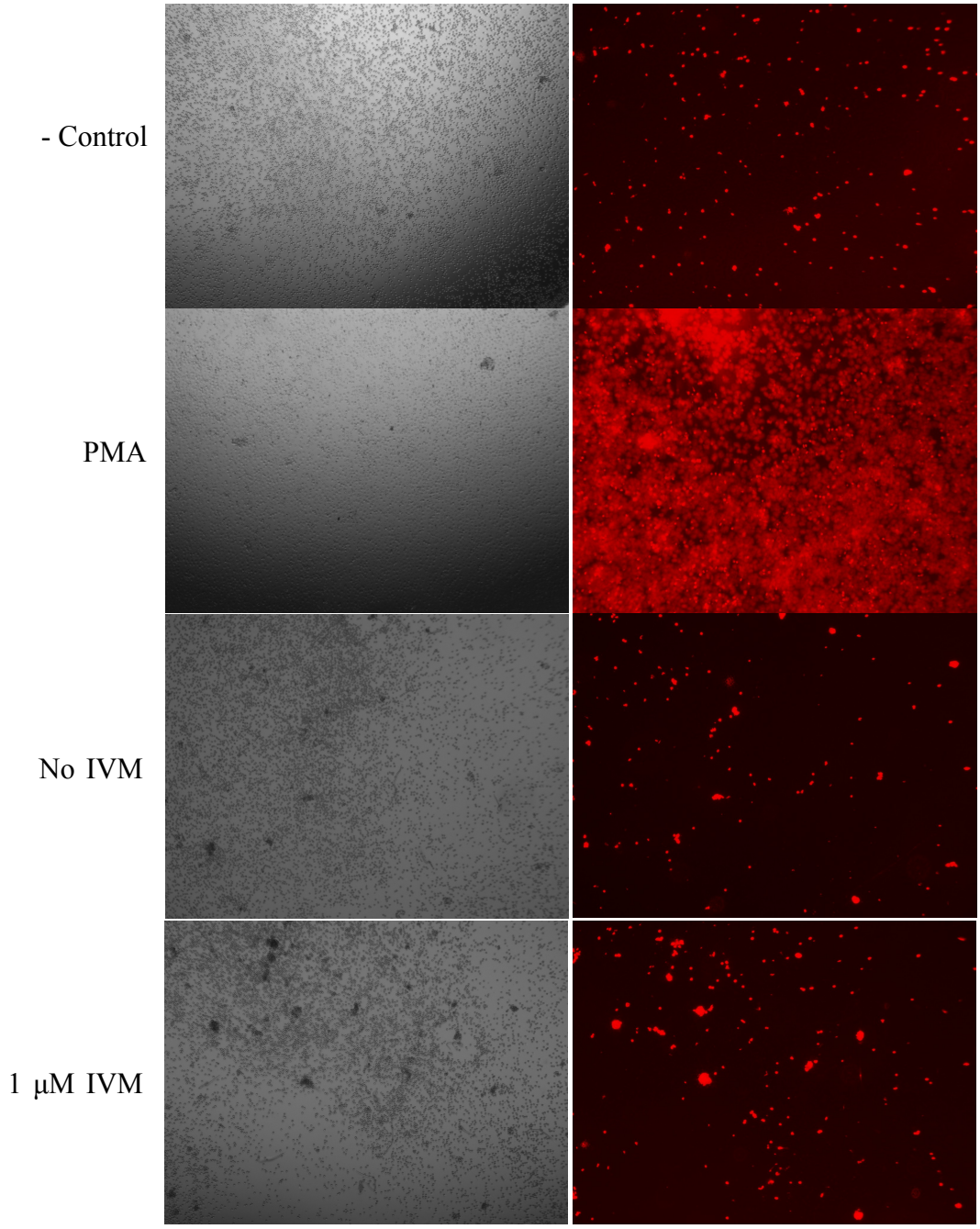

Figure 11: **Normal human neutrophil activation 4-hrs after the addition of neutrophils**. See legend for Figure 10.

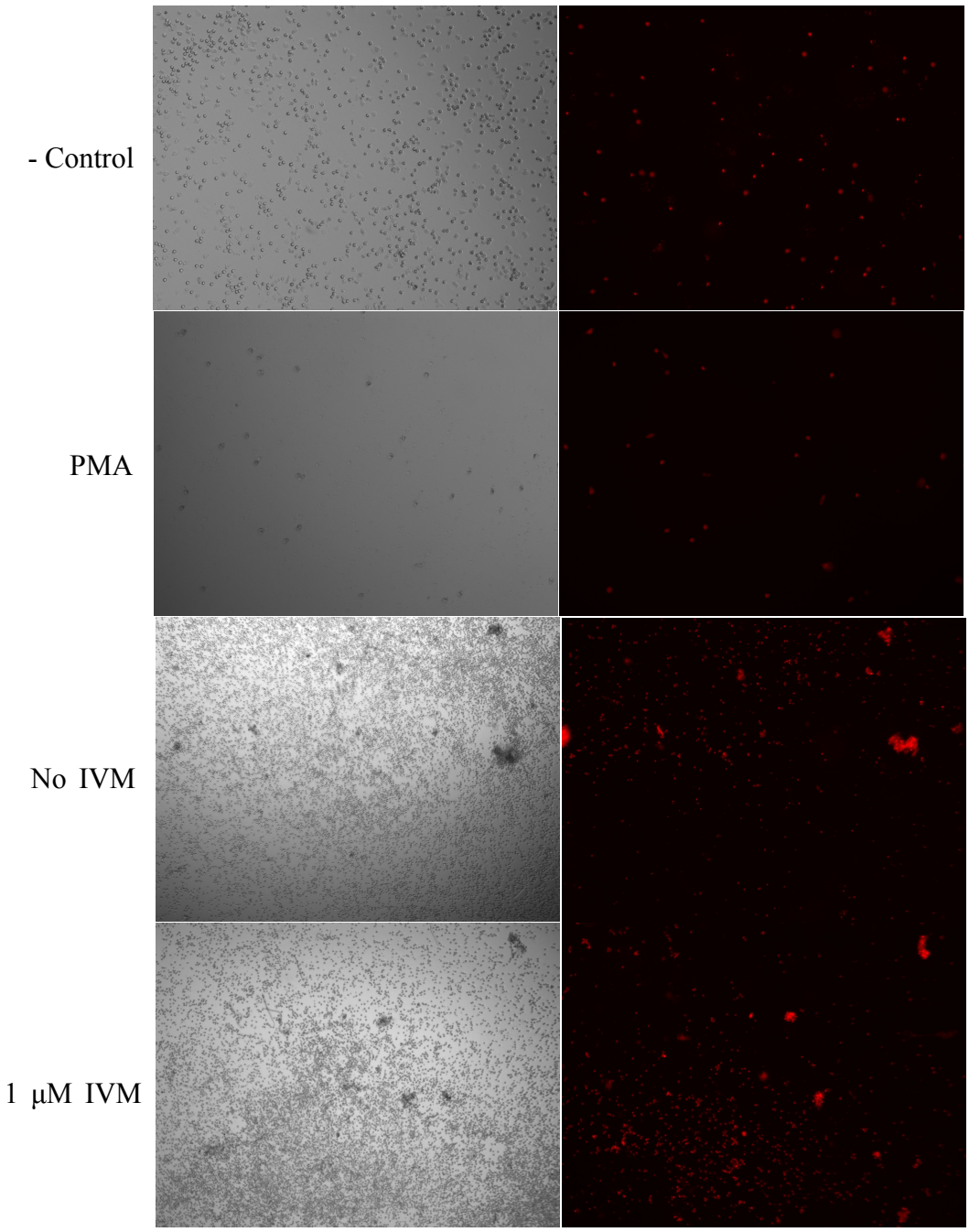

Figure 12: **Normal human neutrophil activation 21-hrs after the addition of neutrophils**. See legend for Figure 10.

In vivo Experiments

To examine the effects of IVM on mf in an *in vivo* model, I assessed parasite numbers and transcript levels, via RNAseq, following treatment of gerbils with multiple doses of IVM (Figure 13).

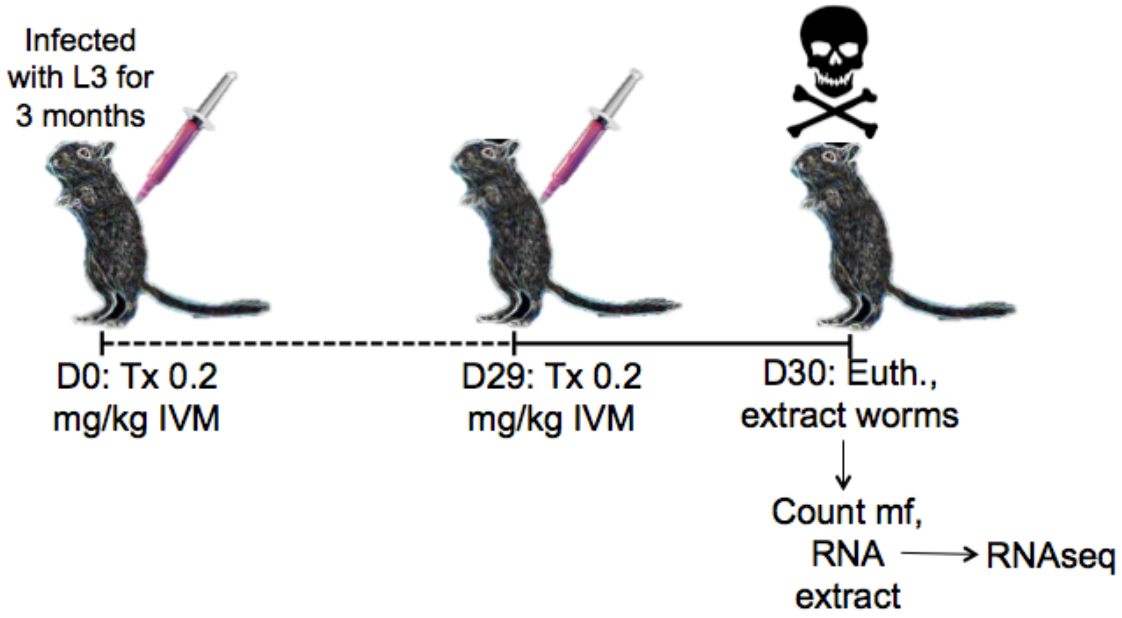

Figure 13: **Timeline for gerbil treatment and RNAseq.**

Upon necropsy of the gerbils used for RNAseq, adult male and female *B. malayi* were separated. Males, females and mf were counted after two and three treatments with IVM (Table 2 and 3).

Table 2: **Quantification of mf, adult males, and adult females from gerbils treated twice with IVM.** Average number of adult control females (n=4) and males (n=4), adult IVM-treated females (n=3) and males (n=3), control mf (n=4) and IVM-treated mf (n=3). $p > 0.05$.

Treated 2X			
	Adult Females	Adult Males	Mf
Control	40	32	1.48E+07
IVM	11	16	1.38E+07

In human LF, one treatment of IVM results in clearance of mf from blood circulation, however, no significant difference was seen between the Control and IVM-treated numbers of mf, even after two treatments with a standard dose of IVM. Despite the lack of clearance of mf in this gerbil model, there was a noticeable difference amongst adults. There were four times more adult females in the Control group than in the IVM-treated group and twice as many Adult Control Males than Adult IVM-treated Males. There were almost three times as many control adults when compared with IVM-treated adults overall (Table 2). However, these numbers were not considered statistically significant.

Table 3: **Quantification of mf, adult males, and adult females from gerbils treated three times with IVM.** Average number of adult control females (n=4) and males (n=4), adult IVM-treated females (n=4) and males (n=4), control mf (n=4) and IVM-treated mf (n=4). $p > 0.05$.

Treated 3X			
	Adult Females	Adult Males	Mf
Control	62	42	1.10E+07
IVM	23	26	8.24E+06

As with the gerbils treated twice, no real difference in mf was observed after three treatments with IVM. Again, there were more adults from the Control gerbils than from the IVM-treated gerbils. There were almost three times as many Control Adult Females than IVM-treated Adult Females and almost twice as many Control Adult Males when compared with IVM-treated Adult Females. Overall, there were twice as many Control Adult *B. malayi* as there were IVM-treated Adults following three treatments with IVM., but again this was not statistically significant(Table 3).

RNAseq

Good RNA quality is imperative for Next Generation Sequencing. In order to measure the quality of extracted RNA, samples were sent to GGF for analysis on an Agilent 2100 Bioanalyzer..

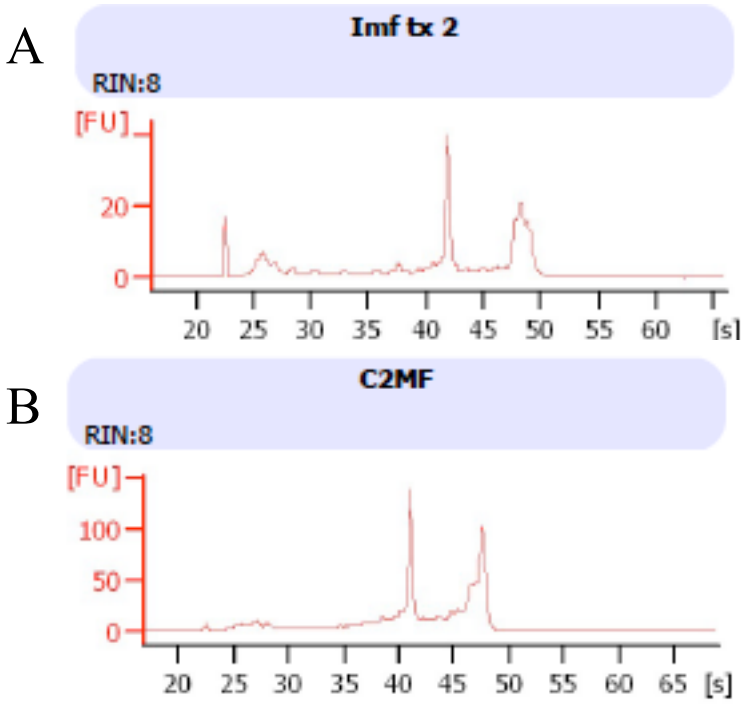

Figure 14: **Agilent Bioanalyzer RNA Electropherograms.** A) RNA from mf extracted from a gerbil treated with two standard doses of IVM (Imf tx2). B) RNA from mf extracted from a gerbil treated with the vehicle control (C2mf).

Both the IVM-treated mf RNA (Figure 14 A) and Control mf RNA (Figure 14 B) displayed the characteristic eukaryotic ribosomal 18S band around 40 seconds and 28S band around 50 seconds. This indicates that these two samples are eukaryotic RNA. Both samples also have an RNA integrity number (RIN) of 8 out of 10 suggesting the RNA was mostly intact and both were used in RNAseq analysis.

RNAseq analysis revealed the total number of reads, number of transcripts assembled from those reads, percentage of transcripts that mapped to the *B. malayi*

reference genome, number of transcripts significantly differentially expressed, and the number of significant genes that were nematode specific and had a putative or known function (Table 4). Some gene products appeared to be represented by multiple transcripts; examples included antifreeze peptide 4, sialin, senescence associated protein, nuclear hormone receptor, and heat shock protein 70 (HSP70). Duplicates were aligned using Geneious v 6.1 to determine if they were unique (Figure 15), or may have been derived from multiple gene copies. Of the HSP70-transcripts three out of 10 were < 95% identical. Both nuclear hormone receptor transcripts were encoded by separate genes. Of 11 senescence associate protein-transcripts, five were from distinct genes. Both sialin transcripts were considered as separate gene products. Of the eight antifreeze peptide 4-transcripts, two of them were from distinct genes.

Table 4: **Statistics from RNAseq analysis of Control and IVM treated mf samples.** Tophat v2.0 and Cufflinks revealed number of reads and transcripts and the percentage of transcripts that mapped to the *B. malayi* genome. BLAST queries and Geneious alignments generated the number of nematode-specific genes and those with a putative/known function.

Total number of reads	35 million / 75 million
Total number of transcripts	23,600 / 24,512
% mapped to reference genome	38% / 68%
Significant differentially expressed transcripts	106
Nematode-specific genes	74
Genes with putative/known function	59

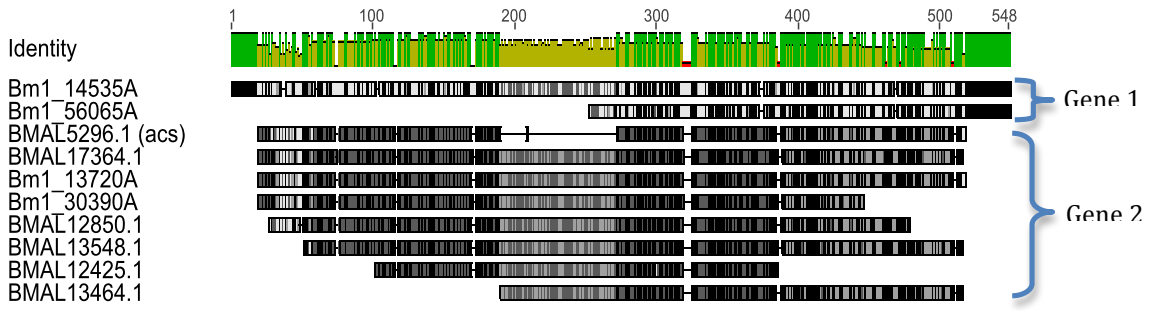

Figure 15: **HSP70 alignment of transcripts reveals two genes.** BLAST queries revealed 10 transcripts with HSP 70 identity. Alignment was performed with default parameters set by Geneious. Transcripts with 95% identity were considered the same. This is representative of alignments for antifreeze peptide 4, sialin, and senescence associated protein. Color coding for mean pairwise identity over all pairs: green is 100% identity, greeny-brown is between 30% and 99% identity, and red is below 30% identity.

The completed analysis resulted in a list of significantly differentially expressed up- and down-regulated genes with possible known functions. In order to confirm these results, a subset of these genes were studied further, using quantitative real-time PCR to measure transcript abundance in the two mRNA populations (Table 5).

Table 5: **RNAseq up- and down-regulated genes.** According to RNAseq analysis these are the most up- and down-regulated significantly differentially expressed genes in the IVM-treated mf sample when compared with Control mf sample.

Down Regulated in Imf Tx2 treated mf	Fold Change
HSP70	4130
Pelxin A	17.28
Chromodomain-helicase-DNA-Binding Protein	13.44
Unc 25 (GAD)	9.19
NHR 10, Ecdysone induced protein 78C	9.98
Up Regulated in Imf Tx2 treaetd mf	**Fold Change**
Shell Matrix protein	3.13
Unc 89 (Locomotion, pharyngeal muscle)	2.59
ER mannosyl-oligosaccharide mannosidase	2.21
Unc 54 (muscle regulation, locomotion and egg laying)	2.04
Unc 68/ Ryanodine receptor (Body tension and locomotion)	1.98

RT-PCR

Primers, designed to amplify up- and down-regulated transcripts identified by the RNAseq analysis, were used for RT-PCR and qPCR (Table 6). Products from RT-PCR were run on a 2% agarose gel to ensure only one product, per primer set, of the correct size was amplified before continuing on to qPCR (Figure 16).

Table 6: **Primer sequences for RT-PCR and qPCR.** Primers were designed according to the most up-and down-regulated transcript sequences. β-tubulin was included as an internal control and the primer was designed from sequence AY705382.

Seq Name	Seq 5' to 3'
nhr-10 fw	GTTCCCTATTGGTGGGTGAA
nhr-10 rv	CAGGGATAACTGGCTTGTGG
Unc-25 fw	GCGCTTCCCAAGATGTAAAC
Unc-25 rv	TACAGCTGCTGCTCCTTTGA
ChromoHel fw	ATGCTGAGGAAGCTGAAGGA
ChromoHel rv	CCACTGGTGCTAGCCTCTTC
Plexin A fw	ACCAGCATCACCTGCACTGT
Plexin A rv	AAGCTGAGGTTTCCATGCAC
HSP-70 fw	CCAGGCGAAGATAAGGATGA
HSP-70 rv	CTGATTAATGTGGGGAGGA
ShellMat fw	ATGATGGCGATGAGAATGGT
ShellMat rv	ATCCGCATTATCGTCCTCAC
Unc-89 fw	AACGGAATCTGAAGCAATGG
Unc-89 rv	TCCGGAACAACACATTCAAA
ERManno fw	CAAACATGCCTGGAAAGGAT
ERManno rv	CGTAACCGGCTTCAAATGAT
Unc-54 fw	CGTGTTGCAGAGATGGAAGA
Unc-54 rv	GACTTGCCATTTCTCCTTGC
Unc-68 fw	ACATCATGCTGCACTTCTCG
Unc-68 rv	GGTGGTGGAAGTTCACGAGT
66 fw	GCAATCCGATCAAATCCTGT
66 rv	CTCCCGGTTCACTCTTGAAA
β-tubulin fw	GCAACTATTCCGACCTGAC
β-tubulin rv	CCTGAAGACAATCGCATCC

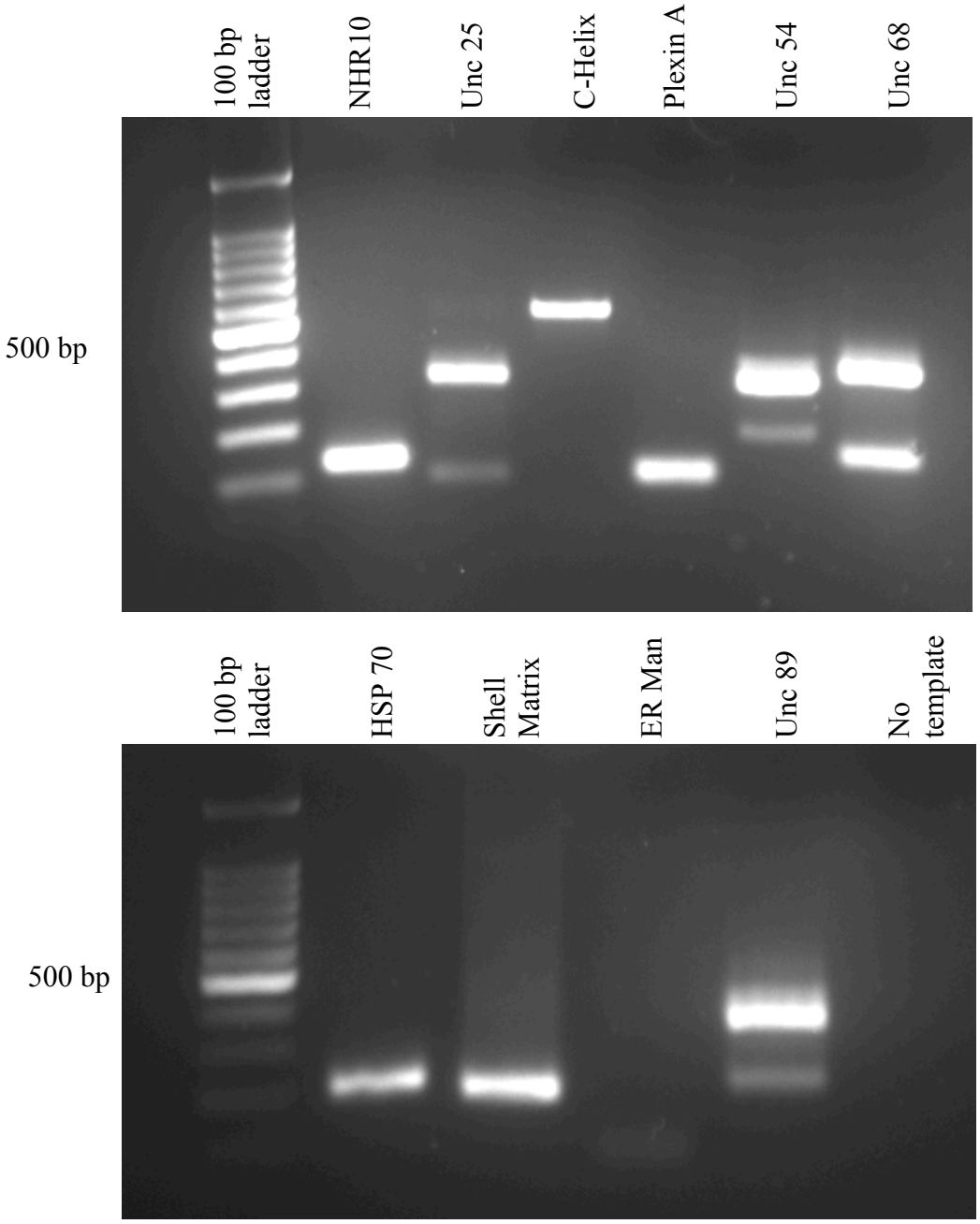

Figure 16: **RT-PCR results of up- and down-regulated primers.** Top 10 differentially expressed gene PCR products were run on a 2% agarose gel and assessed for the amplification of one product of expected size.

RT-PCR revealed that Unc-25, C-helicase, Unc-54, Unc-68, ER Man, and Unc-89 primer pairs all had non-specific binding resulting in multiple bands or bands of unexpected sizes. NHR10, Plexin A, HSP 70, and Shell Matrix primer pairs all resulted in only one

band of expected size. These primers were used for subsequent qPCR analysis. β-tubulin and "66" , a mammalian fe65 homolog, primer pairs also resulted in a band of the correct size (data not shown).

qPCR

All the amplification reactions were performed with serial dilutions of template to obtain standard curves and amplification efficiencies for analysis of gene regulation (Figure 17).

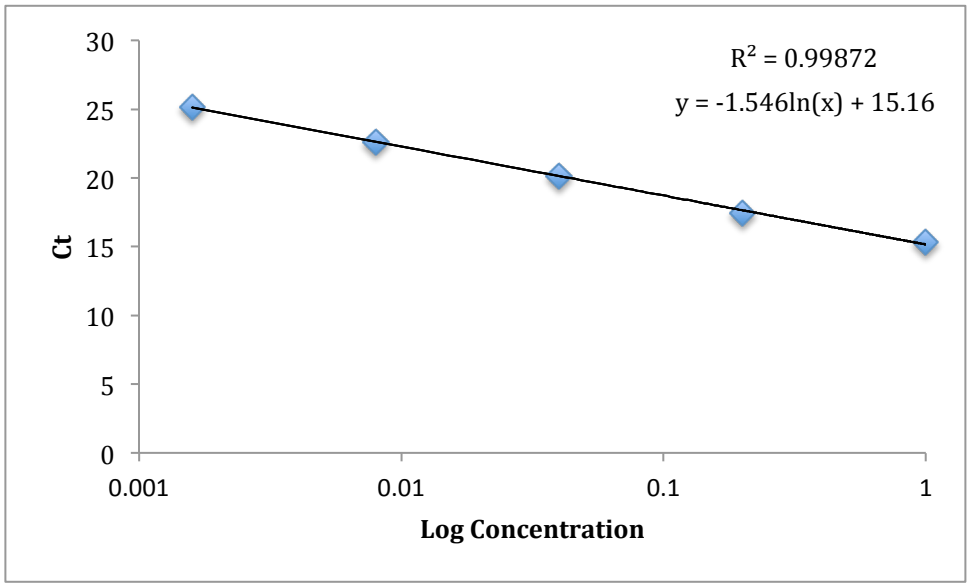

Figure 17: **Standard curve derived from HSP 70 DNA.** Representative of NHR10, Plexin A, Shell Matrix, 66, and β-tubulin standard curves.

One way of corroborating the gene expression results from the RNAseq experiment is by performing qPCR analysis as another form of measuring gene expression between two samples. Unfortunately, the IVM-treated sample (Imf tx 2) used for RNAseq analysis was depleted before qPCR. Another sample (Imf tx 2 #2), aliquoted from the same mf,

was used for qPCR analysis. The RIN of the new IVM-treated sample was 7.9 and considered sufficient for qPCR analysis. Figure 18 A and B are representative of the amplification plots and gel products associated with of all samples. All amplification plots showed consistency amongst replicates, per primer set, and all amplified products revealed one band. Comparisons of qPCR differential gene expression were plotted using REST 2009 and the program calculated efficiencies. Unexpectedly, the results from qPCR did not correlate with the results of the RNAseq experiment (Figure 19 and Table 7).

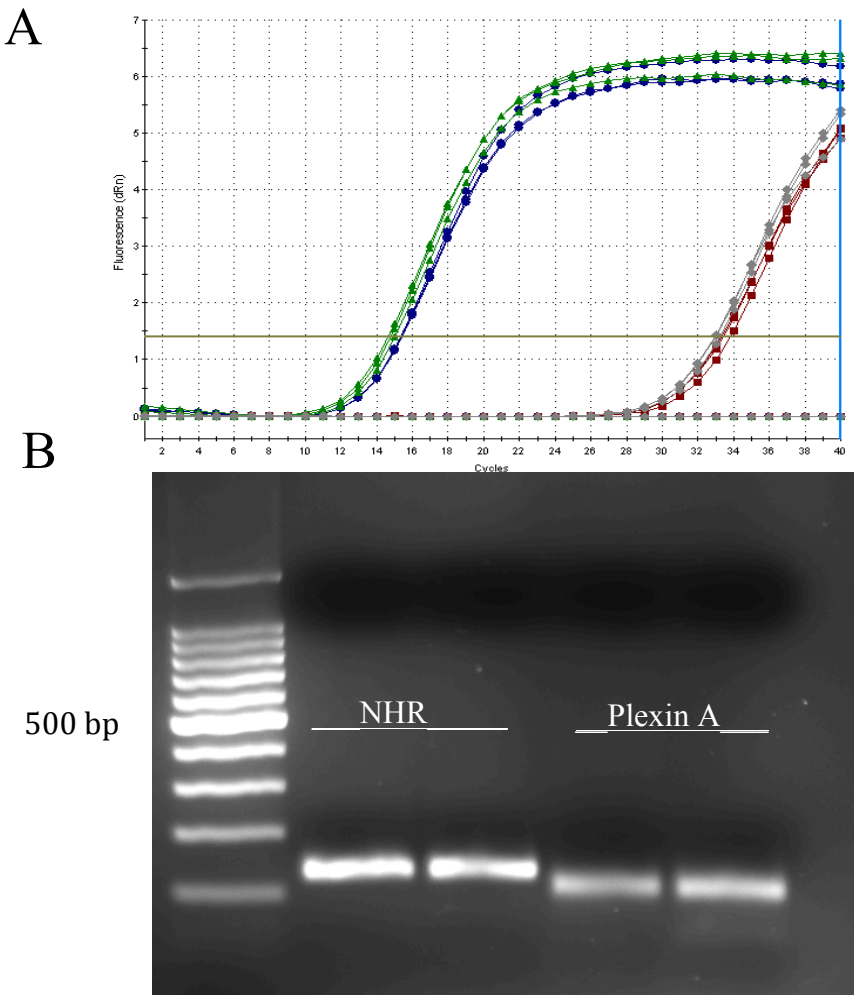

Figure 18: **qPCR results from amplification of NHR 10 and Plexin A Control and IVM-treated DNA.** A) Amplification plot of Control NHR 10 (blue), IVM-treated NHR 10 (green), Control Plexin A (red), and IVM-treated Plexin A (gray). B) Gel from amplified product in Figure A. All amplifications were performed in triplicate.

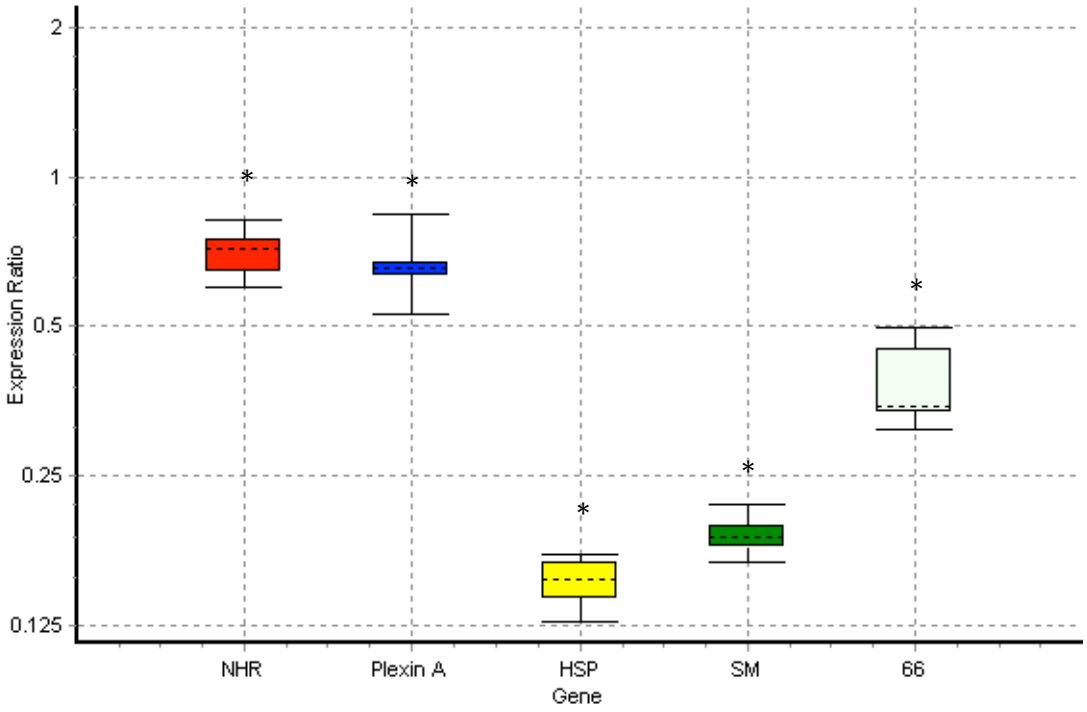

Figure 19: **Relative expression of IVM-treated mf (Imf tx 2 # 2) to Control mf (C2mf).** Expression is relative to the housekeeping β-tubulin gene. This sample is not the same sample sent for RNAseq analysis, but is an aliquot from the same RNA extraction. * $p < 0.05$

Table 7: **Comparison of differential expression of genes between RNAseq analysis and qPCR analysis.** The control RNA sample for both methods was C2mf. The IVM-treated sample for RNAseq was Imf tx2 and for qPCR it was Imf tx2 #2.

Gene Name	RNAseq Fold Change	qPCR Fold Change
NHR	-9.98	-1.42
Plexin A	-17.28	-1.52
HSP 70	-4130	-6.45
Shell Matrix	+ 3.13	-5.26
66	0	-2.65

The discrepancies between the two methods in gene expression could be sample-dependent and not drug-dependent. Since resources prevented analyzing biological replicates in the RNAseq analysis, qPCR was performed on multiple treated and

untreated samples to determine if there is similarity between treatment groups (Figure 20 and 21).

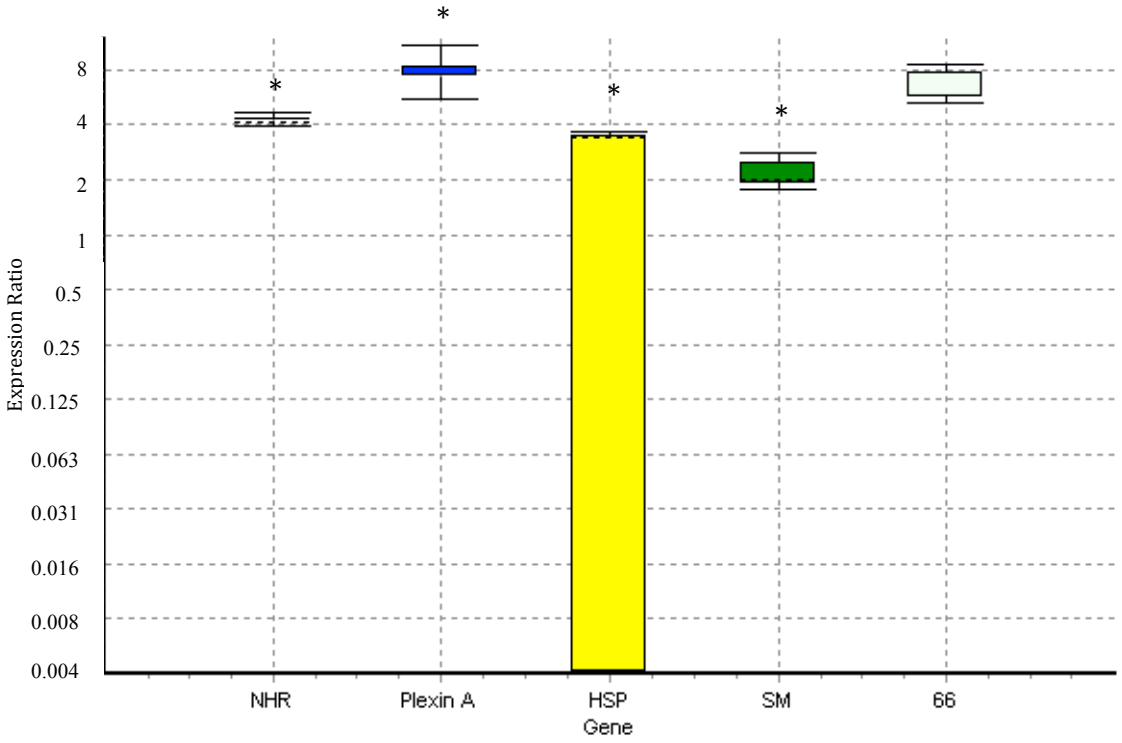

Figure 20: **Relative expression of two control *B. malayi* genes.** Comparison of two control mf samples. * $p < 0.05$

The NHR, Plexin A, and Shell matrix (SM) are up-regulated while HSP 70 has wide variability and is down regulated in one control mf sample compared to another. No significance was seen for the "66" gene (Figure 20). When comparing expression between two IVM-treated mf samples you can see a down-regulation in NHR and Plexin A and an up-regulation in HSP and SM, while no significant difference is seen for "66." There is also notable variability in the SM group (Figure 21). These results indicate that there is no real predictable pattern between treatment groups and that there is a high level of variability that is sample-dependent and not necessarily drug-dependent.

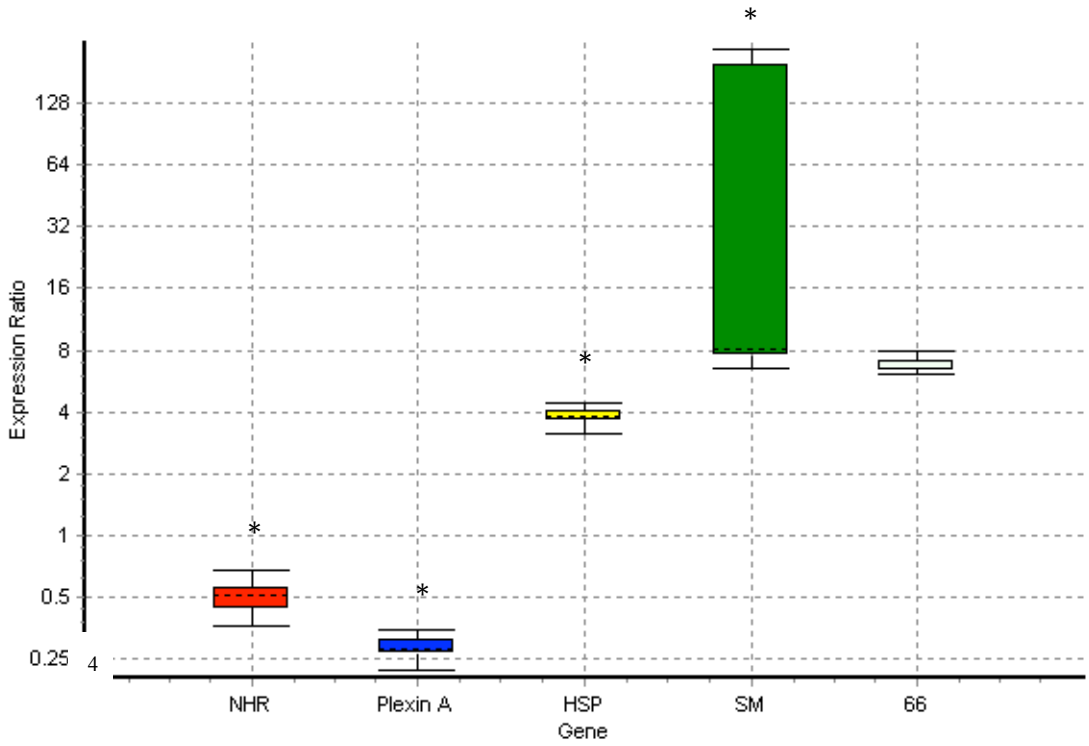

Figure 21. **Relative expression between two IVM-treated mf samples.** qPCR differential expression relative to β-tubulin. * $p < 0.05$.

CHAPTER 5

DISCUSSION

In this study, I assessed the motility of *B. malayi* mf when exposed to varying concentrations of IVM *in vitro*. Previous reports on the effects of IVM *in vitro* show that the concentration required to paralyze the majority of the mf is well above therapeutic doses (Tompkins et al 2010). To assess this we modified scoring systems, developed previously, to score the motility of the mf based on the degree of paralysis elicited by IVM concentrations, 0.1 nM to 10 μM, of IVM (Khunkitti et al 2000, Zaridah et al 2001). The results of the motility assay revealed an EC_{50} of 3-4 μM and 100% paralysis at 10 μM, which is consistent with previous findings (Figure 6). The results of this assay revealed a 100-fold increase of IVM required for paralysis *in vitro* when compared to the 100 nM peak-plasma concentration reported to elicit mf clearance *in vivo* (Edwards et al 1988, Merck & Co. 2002). This suggests that the paralysis by IVM alone is not sufficient to explain the removal of mf from the circulation, therefore, some other factor must be involved. One possibility is that IVM has some effect on the interaction between the parasite and the host's immune system.

Previous studies have been performed to assess the effect of IVM on protein secretion by mf, and the effects of *B. malayi* on various cells of the immune system (Moreno et al 2010, Schroeder et al 2012). Live mf have been shown to inhibit transendothelial migration of neutrophils and monocytes, suggesting that they secrete factors that modulate the functions of these cells. Ivermectin has been shown to decrease

protein secretion that is likely to be required for this immunomodulation. There are also unpublished data showing IVM-dependent neutrophil attachment to a closely related filarial worm, *Dirofilaria immits,* the canine heartworm (Vatta, A., personal communication). Given these findings we hypothesized that treatment of *B. malayi* mf with IVM, *in vitro,* might allow neutrophils to attach to the mf and result in mf killing. We developed a neutrophil attachment assay, in which we exposed mf to IVM, added human neutrophils and autologous serum, and counted the number of mf with at least one neutrophil attached (Figure 7 -9). Disappointingly, there was no significant difference in attachment noted between the IVM-treatment concentrations in the presence or absence of serum. There was, however, a decrease in attachment of neutrophils in the assay containing 5% serum when compared to the assay with no serum. This suggests that neutrophil attachment is inhibited by serum and is not drug dependent. This is not surprising when considering the fact that when neutrophils are out of their natural environment they have a short-lived existence and start to spontaneously activate within hours of being extracted from the body. Further experimentation is clearly required to confirm or refute the original hypothesis, that ivermectin treatment inhibits the production of immunomodulatory molecules by *B. malayi* mf.

Despite the lack of drug-dependent attachment seen *in vitro* with *B. malayi* mf, mf are too large to be engulfed by immune cells and neutrophils release granules, and reactive oxygen species into their surrounding environment when activated (Cadman & Lawrence 2010). This mode of action would not require direct attachment to elicit a deadly effect on a parasite. To assess neutrophil activation, I developed a fluorescence assay in which an impermeable DNA dye bound to the DNA of neutrophils with

compromised cell structures, giving a visual representation of cell activation and death in response to mf and IVM. After inspection of fluorescence at various time points (Figures 10 -12), four hours was selected for the assay due to full activation of neutrophils stimulated with PMA for our positive control (Figure 11). Subsequent analysis of wells containing mf, human neutrophils, 5% autologous serum, with or without 1 μM IVM, at four hours revealed spontaneous activation in the negative control wells, which was expected. The two control wells were the only wells that did not contain mf, and thus provided a reference for activation with no intentional stimulus and with full stimulation. As expected, the cells in wells containing PMA were fully activated in response to the mitogen. The wells containing mf, but no IVM showed a decrease in fluorescence, compared to all other conditions, suggesting that the mf were acting to decrease activation of neutrophils. In wells containing mf plus 1 μM IVM, the results were similar to the negative control well. This suggests that, while IVM does not account for activation over baseline, it does reduce the suppression of activation seen in the presence of mf. One concern is that the scoring of this assay is somewhat subjective and a quantitative analysis of activation is required to provide a more definitive answer. However, these visual observations are consistent with the idea that IVM can decrease the immune modulation by *B. malayi* mf.

Since the completion of the *B. malayi* genome sequence (Ghedin et al 2007), transcriptomic and proteomic studies have shed light on expression of gene and protein levels of various life stages of *B. malayi,* especially in reference to the ES pore and subsequent studies demonstrating immunomodulation (Bennuru et al 2009, Choi et al 2011, Hewitson et al 2009, Li et al 2012, Moreno & Geary 2008). Previously, there had

been no transcriptomic analysis of mf that had been treated with IVM *in vivo*. We hypothesized that IVM treatment of gerbils, infected intraperitoneally with *B. malayi* mf, might result in a decrease in mf production, similar to that seen in human infections, and also change the expression of genes required for the drug to function. Such genes might include those controlling muscle function of the ES pore, those coding for immunomodulatory proteins secreted from the ES pore, ion transport associated with the target of IVM, and those associated with the secretion pathway.

There was no significant difference in the numbers of mf in the peritoneal cavities of the two treatment groups of gerbils. There was an insignificant ($p > 0.05$) decrease in the number of adult male and female worms in the peritoneal cavity of the gerbils treated with IVM (Table 2 & 3). There was evidence of granulomas, indicating that adult worms could be dying, but there was no difference in these observations between the two treatment groups and there has been no evidence in the literature to suggest that IVM treatment elicits macrofilaridical effects in the human infection. This result could be indicative of a robust immune response in the gerbil peritoneum that could result in macrofiliaricidal effects. One other possibility is that this could be attributed to variability in the patency of infection from gerbil to gerbil. Taking together the mf and adult numbers, it is possible, that even though the gerbil model is a permissive one and the most convenient to use, it does not mimic a natural infection in humans.

Despite no effects on worm numbers, the main focus of this study was to assess the effects of IVM on the mf. Of the ~11,500 genes in the *B. malayi* genome, we were most interested in those involved in protein secretion, ion transport, immunomodulation, and detoxification. Gene ontology terms (GO terms) are a good way of identifying genes

and gene product attributes and can be useful in searching for genes involved in specific processes (Ontology 1999). When evaluating the *B. malayi* gene table from Nematode.net, GO terms of interest in the biological process column included intracellular protein transport (Rab-30), protein folding (cyclophilin, chaperonin-60, heat shock proteins), vesicle mediated transport (sec-1 like protein, clathrin, syntaxin), regulation of transcription (zinc finger, nuclear hormone), ion transport, immune response (interleukin enhancer binding factor 2), as well as many others. Analysis between the two treatment groups revealed 106 transcripts that were significantly differentially expressed. Few were in the categories of interest: nuclear hormone receptor, cyclophilin, zinc finger protein, heat shock protein etc. We focused on the most regulated transcripts for further analysis (Table 5). The most striking result was a down regulation of heat shock protein (HSP) 70, also known as binding immunoglobulin protein (BiP), by over 4000-fold. HSP 70 is a chaperone that has been shown to be involved in protein folding of newly synthesized proteins, membrane translocation of organellar and secretory proteins, and control of the activity of regulatory proteins (Mayer & Bukau 2005). The role of this protein in protein folding and translocation of secretory proteins suggests that IVM affects secretory functions in mf. This could lead to a reduction in release of proteins from the ES pore and reduce the production of immunomodulatory proteins. Of the other down-regulated proteins, another of interest is NHR-10, which, according to the GO term, is involved in regulation of transcription, and thus could cause a decrease in the transcription stage of the secretion pathway. GAD, an enzyme that catalyzes glutamate to GABA, is also down-regulated in the IVM-treated mf. GABA-gated chloride receptors are also a target for avermectins, such as IVM, and are

known to be involved in nematode locomotion. The decrease in this enzyme could conceivably play a role in paralysis of mf (Merck & Co. 2002, Wolstenholme & Rogers 2005). The up-regulated genes are less diverse than the down-regulated ones, and mostly comprise genes that are involved in locomotion and muscle regulation. This suggests that these functions are at least somewhat affected by drug treatment. More biological replicates would be needed to evaluate the true transcriptomic profile of mf treated with IVM.

In order to validate the RNAseq results, qPCR analysis was performed on several different RNA samples for some of the most differentially expressed genes (Table 6, Table 7, and Figure 19 -21). Of the two RNA samples used for RNAseq analysis, the IVM-treated sample was depleted and could not be used for qPCR. In its place, an equivalent sample from the same batch of mf was used. Figure 19 represents the differential expression between the control mf sample used in RNAseq analysis and the second IVM-treated sample. Table 7 shows that there is a significant discrepancy between the RNAseq output and the qPCR output. qPCR suggests that many of the genes thought to be differentially expressed may not be. This could be attributed to the fact that there could be multiple copies of the same gene. This can be seen in the gene alignment for HSP 70 in which two distinct genes can be seen, each with splice variants (Figure 15). RNAseq analysis revealed a down-regulation of over 4000-fold while qPCR is just over 6-fold. One possibility is that RNAseq analysis picked up the expression levels for one copy of this gene and qPCR amplified the other copy of the gene. Sequencing of these two products could provide insight into this discrepancy. Another possibility stems from the fact that the IVM-treated samples were not the same in both analyses and there could

be variability between samples, even if they have been treated as similarly as possible. From the qPCR data of other RNA samples, it is evident that there is variability between samples within the same treatment group. Ideally when comparing two control mf samples, there would be no up- or down-regulation amongst the genes, yet four out of five genes examined were significantly differentially expressed between such samples (Figure 20). Even between two IVM-treated mf samples there are significant differences in the expression of four out of five genes (Figure 21). All of these results combined, give a strong indication that there is a great deal of variability between mf within treatment groups. These results reiterate the importance of biological replicates in analysis of assays with high levels of variability, especially when observed in multiple aspects of experimental design. Unfortunately, no definitive conclusions can be made from the RNAseq data and the qPCR data without performing the studies again with multiple biological replicates.

In this study I have demonstrated that the concentration of IVM required *in vitro* to paralyze 100% of *B. malayi* mf is much higher than what causes mf clearance in human infections, suggesting a role of the immune system in mf clearance. My studies involving neutrophil attachment did not suggest a drug-dependent effect, but observational analysis of neutrophil activation, when exposed to mf and IVM, implies that IVM could play a role in decreasing immune modulation in the host. Further studies, quantifying neutrophil activation, could provide a better understanding of the role of IVM. No definitive conclusions can be made about the effects of IVM on transcription of certain genes, but further analysis with multiple samples would give a more definitive answer as to how IVM regulates gene transcription and protein secretion. From the

results of this study and previous studies I have developed a working model for further investigation (Figure 22 and 23). It suggests that IVM treatment results in the clearance of mf from the circulation through a combination of effects on both the parasite and the host immune system. This is not entirely novel, as it is well known that the anti-schistosome activity of praziquantel is dependent on an intact immune system. These findings could result in a better understanding of the mode of action for IVM in a human infection and could help prepare for any developing resistance in parasites causing lymphatic filariasis.

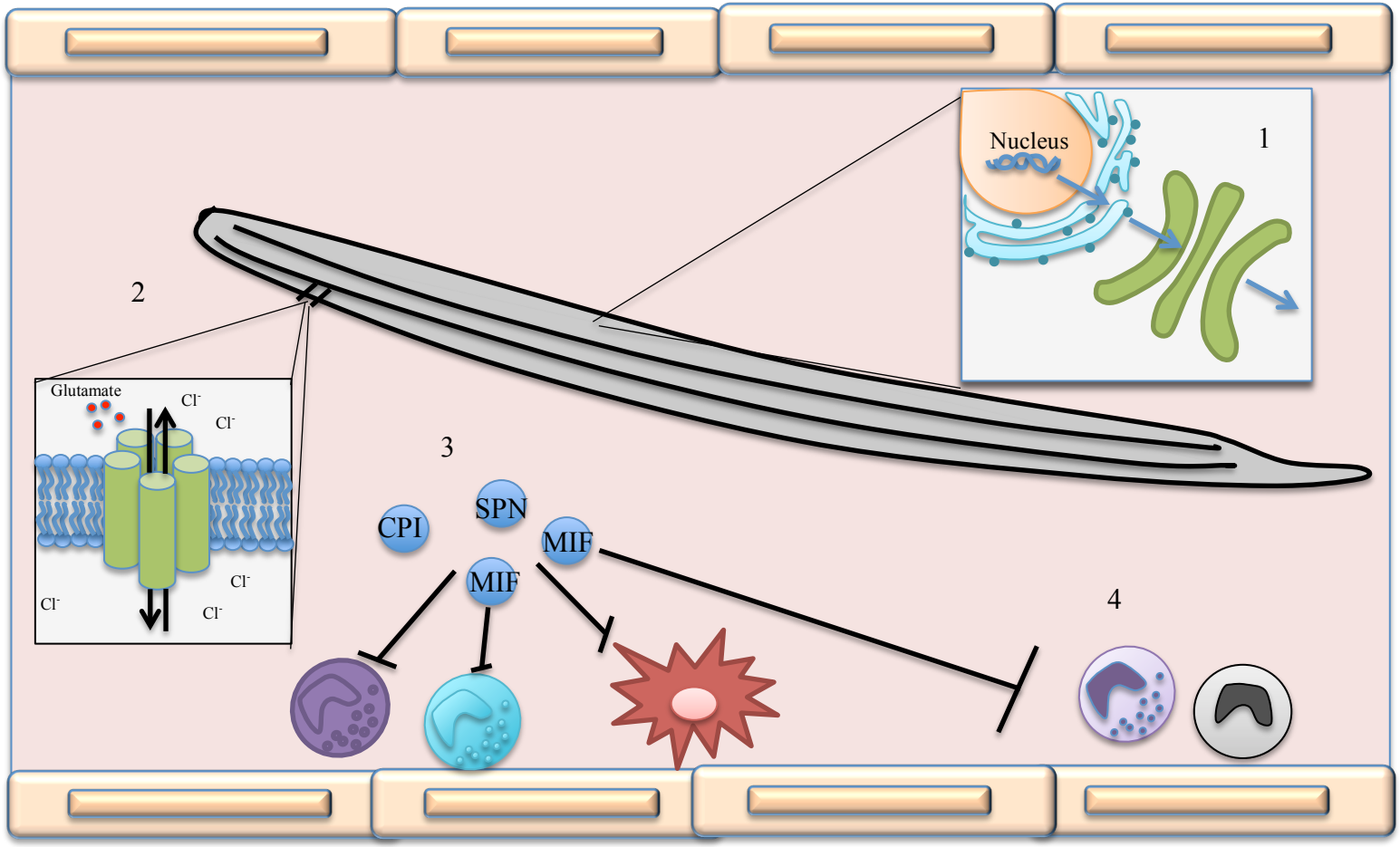

Figure 22: **Proposed model for immunomodulation by *B. malayi* mf.** 1. Nascent protein from the nucleus is moved into the rough ER where chaperones ensure proper folding for secretion. They then move to the Golgi for transport outside of the cell. 2. A functional GluCl allows ES proteins to be released through the ES Pore. 3. Immunomodulatory proteins inhibit activation of granulocytes, DC, and macrophages. 4. Immunomodulatory proteins also inhibit transendothelial migration of neutrophils and monocytes. The infection remains unrecognized by the host's immune system.

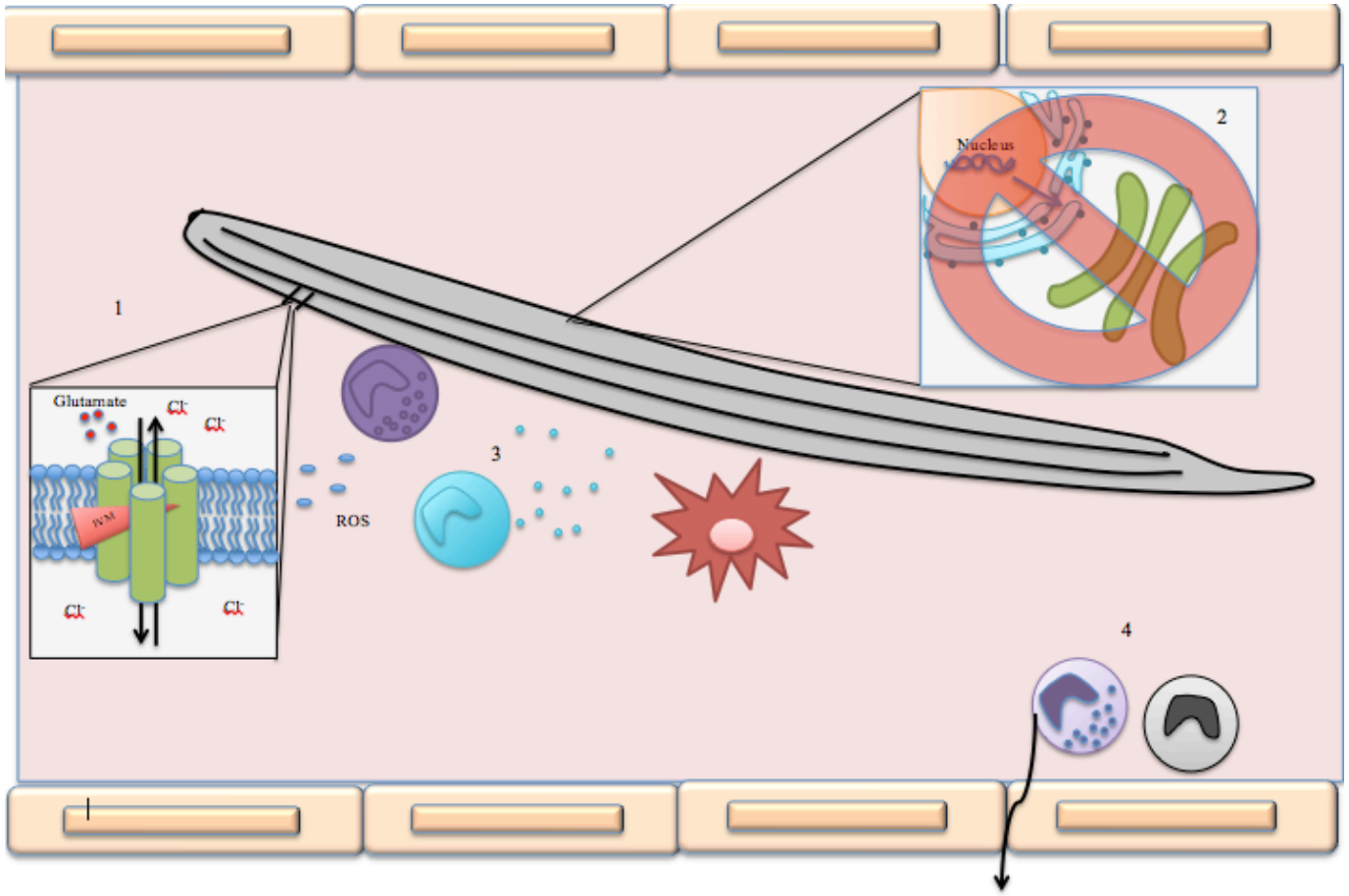

Figure 23: **Proposed mode of action of IVM on mf immunomodulation.** 1. IVM binds to AVR-14, on the muscles surrounding the ES pore, inhibiting protein secretion through an unknown mechanism. 2. The secretion pathway is inhibited, resulting in transcriptional regulation of genes required for secretion of proteins. 3. Immune cells recognize the mf and attack with granzymes and ROS, leading to their removal from circulation. 4. Neutrophils and monocytes extravasate to areas of inflammation to help fight infection.

REFERENCES

2012. Global programme to eliminate lymphatic filariasis: progress report, 2011. *Releve epidemiologique hebdomadaire / Section d'hygiene du Secretariat de la Societe des Nations = Weekly epidemiological record / Health Section of the Secretariat of the League of Nations* 87: 346-56

Arndts K, Deininger S, Specht S, Klarmann U, Mand S, et al. 2012. Elevated adaptive immune responses are associated with latent infections of Wuchereria bancrofti. *PLoS neglected tropical diseases* 6: e1611

Babu S, Bhat SQ, Pavan Kumar N, Lipira AB, Kumar S, et al. 2009. Filarial lymphedema is characterized by antigen-specific Th1 and th17 proinflammatory responses and a lack of regulatory T cells. *PLoS neglected tropical diseases* 3: e420

Babu S, Nutman TB. 2003. Proinflammatory cytokines dominate the early immune response to filarial parasites. *Journal of immunology* 171: 6723-32

Bennett JL, Williams JF, Dave V. 1988. Pharmacology of ivermectin. *Parasitology today* 4: 226-8

Bennuru S, Semnani R, Meng Z, Ribeiro JM, Veenstra TD, Nutman TB. 2009. Brugia malayi excreted/secreted proteins at the host/parasite interface: stage- and gender-specific proteomic profiling. *PLoS neglected tropical diseases* 3: e410

Boatin BA, Basanez MG, Prichard RK, Awadzi K, Barakat RM, et al. 2012. A research agenda for helminth diseases of humans: towards control and elimination. *PLoS neglected tropical diseases* 6: e1547

Bourke CD, Maizels RM, Mutapi F. 2011. Acquired immune heterogeneity and its sources in human helminth infection. *Parasitology* 138: 139-59

Boyd A, Bennuru S, Wang Y, Sanprasert V, Law M, et al. 2013. Quiescent innate response to infective filariae by human Langerhans cells suggests a strategy of immune evasion. *Infection and immunity* 81: 1420-9

Brown KR, Ricci FM, Ottesen EA. 2000. Ivermectin: effectiveness in lymphatic filariasis. *Parasitology* 121 Suppl: S133-46

Cadman ET, Lawrence RA. 2010. Granulocytes: effector cells or immunomodulators in the immune response to helminth infection? *Parasite immunology* 32: 1-19

CDC. 2013. B. malayi Life Cycle. pp. Life cycle image of B. malayi

Choi YJ, Ghedin E, Berriman M, McQuillan J, Holroyd N, et al. 2011. A deep sequencing approach to comparatively analyze the transcriptome of lifecycle stages of the filarial worm, Brugia malayi. *PLoS neglected tropical diseases* 5: e1409

Collingridge GL, Olsen RW, Peters J, Spedding M. 2009. A nomenclature for ligand-gated ion channels. *Neuropharmacology* 56: 2-5

Cox FE. 2002. History of human parasitology. *Clinical microbiology reviews* 15: 595-612

Crandall RB, McGreevy PB, Connor DH, Crandall CA, Neilson JT, McCall JW. 1982. The ferret (Mustela putorius furo) as an experimental host for Brugia malayi and Brugia pahangi. *The American journal of tropical medicine and hygiene* 31: 752-9

Cross JH. 1996. Filarial Nematodes In *Medical Microbiology*, ed. S Baron. Galveston (TX)

Crump A, Omura S. 2011. Ivermectin, 'wonder drug' from Japan: the human use perspective. *Proceedings of the Japan Academy. Series B, Physical and biological sciences* 87: 13-28

Cully DF, Vassilatis DK, Liu KK, Paress PS, Van der Ploeg LH, et al. 1994. Cloning of an avermectin-sensitive glutamate-gated chloride channel from Caenorhabditis elegans. *Nature* 371: 707-11

Dent JA, Davis MW, Avery L. 1997. avr-15 encodes a chloride channel subunit that mediates inhibitory glutamatergic neurotransmission and ivermectin sensitivity in Caenorhabditis elegans. *The EMBO journal* 16: 5867-79

Edwards G, Dingsdale A, Helsby N, Orme ML, Breckenridge AM. 1988. The relative systemic availability of ivermectin after administration as capsule, tablet, and oral solution. *European journal of clinical pharmacology* 35: 681-4

Genchi C, Kramer LH, Sassera D, Bandi C. 2012. Wolbachia and its implications for the immunopathology of filariasis. *Endocrine, metabolic & immune disorders drug targets* 12: 53-6

Ghedin E, Wang S, Spiro D, Caler E, Zhao Q, et al. 2007. Draft genome of the filarial nematode parasite Brugia malayi. *Science* 317: 1756-60

Gonzalez Canga A, Sahagun Prieto AM, Diez Liebana MJ, Fernandez Martinez N, Sierra Vega M, Garcia Vieitez JJ. 2008. The pharmacokinetics and interactions of ivermectin in humans--a mini-review. *The AAPS journal* 10: 42-6

Gonzalez P, Gonzalez FA, Ueno K. 2012. Ivermectin in human medicine, an overview of the current status of its clinical applications. *Current pharmaceutical biotechnology* 13: 1103-9

Grenfell BT, Michael E, Denham DA. 1991. A model for the dynamics of human lymphatic filariasis. *Parasitology today* 7: 318-23

Gupta R, Bajpai P, Tripathi LM, Srivastava VM, Jain SK, Misra-Bhattacharya S. 2004. Macrophages in the development of protective immunity against experimental Brugia malayi infection. *Parasitology* 129: 311-23

Hawking F, Gammage K. 1968. The periodic migration of microfilariae of Brugia malayi and its response to various stimuli. *The American journal of tropical medicine and hygiene* 17: 724-9

Hewitson JP, Grainger JR, Maizels RM. 2009. Helminth immunoregulation: the role of parasite secreted proteins in modulating host immunity. *Molecular and biochemical parasitology* 167: 1-11

Horoszok L, Raymond V, Sattelle DB, Wolstenholme AJ. 2001. GLC-3: a novel fipronil and BIDN-sensitive, but picrotoxinin-insensitive, L-glutamate-gated chloride channel subunit from Caenorhabditis elegans. *British journal of pharmacology* 132: 1247-54

Horton J, Witt C, Ottesen EA, Lazdins JK, Addiss DG, et al. 2000. An analysis of the safety of the single dose, two drug regimens used in programmes to eliminate lymphatic filariasis. *Parasitology* 121 Suppl: S147-60

Khunkitti W, Fujimaki Y, Aoki Y. 2000. In vitro antifilarial activity of extracts of the medicinal plant Cardiospermum halicacabum against Brugia pahangi. *Journal of helminthology* 74: 241-6

Li BW, Wang Z, Rush AC, Mitreva M, Weil GJ. 2012. Transcription profiling reveals stage- and function-dependent expression patterns in the filarial nematode Brugia malayi. *BMC genomics* 13: 184

Mayer MP, Bukau B. 2005. Hsp70 chaperones: cellular functions and molecular mechanism. *Cellular and molecular life sciences : CMLS* 62: 670-84

Maizels RM, Yazdanbakhsh M. 2003. Immune regulation by helminth parasites: cellular and molecular mechanisms. *Nature reviews. Immunology* 3: 733-44

McCavera S, Walsh TK, Wolstenholme AJ. 2007. Nematode ligand-gated chloride channels: an appraisal of their involvement in macrocyclic lactone resistance and prospects for developing molecular markers. *Parasitology* 134: 1111-21

Merck & Co. I. 2002. STROMECTOL® (IVERMECTIN) TABLETS. pp. Description of Stromectol drug information

Michalski ML, Griffiths KG, Williams SA, Kaplan RM, Moorhead AR. 2011. The NIH-NIAID Filariasis Research Reagent Resource Center. *PLoS neglected tropical diseases* 5: e1261

Moreno Y, Geary TG. 2008. Stage- and gender-specific proteomic analysis of Brugia malayi excretory-secretory products. *PLoS neglected tropical diseases* 2: e326

Moreno Y, Nabhan JF, Solomon J, Mackenzie CD, Geary TG. 2010. Ivermectin disrupts the function of the excretory-secretory apparatus in microfilariae of Brugia malayi. *Proceedings of the National Academy of Sciences of the United States of America* 107: 20120-5

Nutman TB, Kumaraswami V. 2001. Regulation of the immune response in lymphatic filariasis: perspectives on acute and chronic infection with Wuchereria bancrofti in South India. *Parasite immunology* 23: 389-99

Ontology TG. 1999. pp. Gene ontology terms

Ottesen EA, Vijayasekaran V, Kumaraswami V, Perumal Pillai SV, Sadanandam A, et al. 1990. A controlled trial of ivermectin and diethylcarbamazine in lymphatic filariasis. *The New England journal of medicine* 322: 1113-7

Pang L, Hayes CP, Buac K, Yoo DG, Rada B. 2013. Pseudogout-associated inflammatory calcium pyrophosphate dihydrate microcrystals induce formation of neutrophil extracellular traps. *Journal of immunology* 190: 6488-500

Schroeder JH, Simbi BH, Ford L, Cole SR, Taylor MJ, et al. 2012. Live Brugia malayi microfilariae inhibit transendothelial migration of neutrophils and monocytes. *PLoS neglected tropical diseases* 6: e1914

Scott AL, Ghedin E. 2009. The genome of Brugia malayi - all worms are not created equal. *Parasitology international* 58: 6-11

Shenoy RK, Dalia S, John A, Suma TK, Kumaraswami V. 1999. Treatment of the microfilaraemia of asymptomatic brugian filariasis with single doses of ivermectin, diethylcarbamazine or albendazole, in various combinations. *Annals of tropical medicine and parasitology* 93: 643-51

Tompkins JB, Stitt LE, Ardelli BF. 2010. Brugia malayi: in vitro effects of ivermectin and moxidectin on adults and microfilariae. *Experimental parasitology* 124: 394-402

Vassilatis DK, Arena JP, Plasterk RH, Wilkinson HA, Schaeffer JM, et al. 1997. Genetic and biochemical evidence for a novel avermectin-sensitive chloride channel in Caenorhabditis elegans. Isolation and characterization. *The Journal of biological chemistry* 272: 33167-74

WHO. 2011. pp. Distribution and Status of Preventative Chemotherap for Lymphatic Filariasis, worldwide 2011

Williamson SM, Walsh TK, Wolstenholme AJ. 2007. The cys-loop ligand-gated ion channel gene family of Brugia malayi and Trichinella spiralis: a comparison with Caenorhabditis elegans. *Invertebrate neuroscience* 7: 219-26

Wolstenholme AJ, Rogers AT. 2005. Glutamate-gated chloride channels and the mode of action of the avermectin/milbemycin anthelmintics. *Parasitology* 131 Suppl: S85-95

Wolstenholme AJ. 2012. Glutamate-gated chloride channels. *The Journal of biological chemistry* 287: 40232-8

Yates DM, Wolstenholme AJ. 2004. An ivermectin-sensitive glutamate-gated chloride channel subunit from Dirofilaria immitis. *International journal for parasitology* 34: 1075-81

Zaridah MZ, Idid SZ, Omar AW, Khozirah S. 2001. In vitro antifilarial effects of three plant species against adult worms of subperiodic Brugia malayi. *Journal of ethnopharmacology* 78: 79-84